

**ASSESSMENT OF WATER TABLE FLUCTUATIONS AND
WETLAND DELINEATION BY HYDROLOGIC MODELLING,
BOSQUECITO, NEW MEXICO**

By

Junhao Hu

Submitted in Partial Fulfillment of the Requirements for the Degree of
Master of Science in Hydrology

New Mexico Institute of Mining and Technology

Socorro, New Mexico

July, 2015

ProQuest Number: 1599239

All rights reserved

INFORMATION TO ALL USERS

The quality of this reproduction is dependent upon the quality of the copy submitted.

In the unlikely event that the author did not send a complete manuscript and there are missing pages, these will be noted. Also, if material had to be removed, a note will indicate the deletion.



ProQuest 1599239

Published by ProQuest LLC (2015). Copyright of the Dissertation is held by the Author.

All rights reserved.

This work is protected against unauthorized copying under Title 17, United States Code
Microform Edition © ProQuest LLC.

ProQuest LLC.
789 East Eisenhower Parkway
P.O. Box 1346
Ann Arbor, MI 48106 - 1346

ABSTRACT

In this study, we evaluated what the key factors controlling water table fluctuations within the Bosquecito wetland along the Rio Grande near San Antonio, NM using hydrologic models constrained by field data. In 2010, eight 2-inch diameter wells were installed to a depth of 7 feet along an east-west transect through the Bosquecito wetland. Two additional wells were installed to the north and south of the middle wells (well w4). Groundwater table elevations were recorded using pressure transducers between 2010 and 2014. Manual measurements of water table elevations were also collected manually every 2-4 weeks. Slug tests and a barometric efficiency analysis were performed in several wells to determine specific storage and hydraulic conductivity of the shallow sand aquifer underlying the wetland. The hydraulic conductivity in three wells varied between 5 and 32 m/d. The specific storage coefficient was found to vary between 1.8×10^{-6} and 1.1×10^{-4} 1/m. Evapotranspiration was estimated using Kimberly Penman, Blaney-Criddle methods and Landsat image analysis. Temporal variations in groundwater table elevations were found to be closely correlated with Rio Grande stage. Wells furthest from the river had a relatively smaller amplitude of variation and were about 50 days out of phase with river stage fluctuations. Wells closest to the river showed no phase shift and had a similar amplitude of variation as the river. Average water levels of wells within the wetland were on average, 1 m lower than average river stage suggesting the importance of local groundwater supported evapotranspiration. We constructed a series of one-dimensional hydrologic models to understand the controls of river stage and evapotranspiration on water table elevations in an analysis analogous to Rorabaugh (1964). We found that a hydraulic diffusivity of the shallow sand aquifer underlying the wetland was $9000 \text{ m}^2/\text{d}$ and an average evapotranspiration rate of 0.004 m/d provided a reasonable match to the observed data. We then constructed a three-dimensional, four layer MODFLOW steady state model to understand what are the key hydrologic stresses and aquifer parameters controlling water table fluctuations within and near the wetland. We concluded that a significant proportion of the water table fluctuations were due to changes in river stage. Next we constructed a three-dimensional, four layer MODFLOW transient model of the wetland and surrounding area to assess the effects of vertical leakage across confining units, the presence of regional drains (LFCC), the ET, pumping/irrigation and sinuosity of the Rio Grande on water table elevations. The three dimensional models allowed us to calibrate our model to regional water table maps and Landsat images of evapotranspiration. We used the best fit, simulated groundwater table elevations to delineate the boundaries of the wetland based on Hydric

Soil Technical Standard (2007) (14 days of water table less than 1 foot below the land surface). The wetland area was found to compare well with the locations of hydric soils measured from the sediment cores collected during the drilling of the 8 monitoring wells.

Keywords: Bosquecito, Wetland, Groundwater Modelling, Wetland Groundwater Fluctuations Influential Factors, Wetland Delineation

ACKNOWLEDGEMENTS

Many people have contributed to this project, without their help, this project couldn't be finished. I would express my gratitude and applause to my advisor Mark Person, he is such a dedicated, hardworking and responsible advisor who helped me get in the track of a graduate student life in a foreign country, who helped me and cheered me both in life and study!

I would like to thank my parents as well who gave me strength and encouragement when I felt tired and desperate in reaching the completion of my master degree.

I would thank Aaron Miller (NRCS scientist in Santa Fe) who provided a lot of valuable data which supports this project. Kim Haar who did the field work and recorded a period of the data after Aaron.

I would also thank my classmates and friends, Jeff Pepin for his technical help, Zhidi Wu who assisted me in slug test, Amy Galanter for her encouragement and friendship companion.

TABLE OF CONTENTS

LIST OF FIGURES	vi
LIST OF TABLES	ix
CHAPTER 1 INTRODUCTION	1
1.1 Motivation	1
1.2 Methods of Wetland Delineation	1
1.3 Study Objectives	3
1.4 Prior Hydrological Modeling Studies on Wetland.....	3
CHAPTER 2 STUDY AREA	5
2.1 Location.....	5
2.2 Climate	8
2.3 Geology	9
2.4 Hydrology.....	11
2.4.1 Rio Grande Stage/Discharge	11
2.4.2 Riverbed Conductance.....	13
2.4.3 Low Flow Conveyance Channel.....	13
2.4.4 Agriculture Canals and Drains	14
2.4.5 Arroyos	14
2.4.6 Groundwater Table Elevations	14
2.4.7 Aquifer Tests	16
2.5 Vegetation	17
2.6 Fauna	17
2.7 Previous Hydrological Modeling Studies	17
CHAPTER 3 METHODS	19

3.1 Overview	19
3.2 Field Methods.....	20
3.2.1 Groundwater Table Fluctuation Monitoring.....	20
3.2.2 Hvorslev Slug Test	22
3.2.3 The Specific Storage Estimation	24
3.2.4 Evapotranspiration.....	25
3.2.5 The Pumping/Irrigation Rate Estimation.....	26
3.3 Groundwater Model	27
3.3.1 1D Transient Numerical Model Based on Rorabough Equation	27
3.3.2 Numerical Model in MODFLOW	29
3.3.2.1 Model Domain/Discretization.....	29
3.3.2.2 Boundary Condition.....	30
3.3.2.3 The Rio Grande River Stage	33
3.3.2.4 The Description and Properties of the Low Flow Conveyance Channel...	34
3.3.2.5 MODFLOW Evapotranspiration Module	34
3.3.2.6 Pumping and Irrigation	35
3.3.2.7 Recharge on the Site	35
3.3.2.8 Layer Properties	36
CHAPTER 4 RESULTS	37
4.1 Specific Storage Estimation	37
4.2 Slug Tests	39
4.3 Evapotranspiration	41
4.4 The Pumping/Irrigation Rate Estimation Using Blaney-Criddle Method.....	43
4.5 1D Numerical Model Using Rorabaugh Equation	44
4.6 Three-Dimensional MODFLOW Results	49
4.6.1 Steady State MODFLOW Model	49
4.6.2 Transient Model in MODFLOW	55
4.6.3 Sensitivity Analysis	57
4.6.3.1 Rio Grande Stage	57
4.6.3.2 Riverbed Conductivity	58
4.6.3.3 LFCC Conductivity.....	59
4.6.3.4 Pumping and Confining Unit	60
4.6.3.5 ET Effects	61
4.6.3.6 Regional ET Effects	62

4.7 Influential Factors for the Groundwater Tables in Wetland Side	64
4.8 Hydric Soil and Wetland Delineation Using Simulated Water Table Fluctuation .	65
CHAPTER 5 DISCUSSION.....	67
5.1 Testing of Model Results	67
5.1.1 Surface Water and Dry Area	67
5.1.2 Comparison of the Simulated Water Table Elevations with Hydric Soil Data	69
5.2 Advantage of Hydrological Modeling Approach to Wetland Delineation	70
5.3 Conclusion.....	70
5.4 Recommendation.....	71
REFERENCES	72

LIST OF FIGURES

Figure 1: A. Location of the research site along the Rio Grande near San Antonio, NM. The green dots denote the locations of 10 monitoring wells installed as part of this project. The red stars denote the locations of stream gauge stations along the Rio Grande. B. Boundary of the research site and 3D model domain (thick red line). The low flow conveyance channel (LFCC) is denoted by light blue line. The Rio Grande in the research domain is the black line. Yellow line is the abandoned ditch. Orange lines stand for the arroyos. Purple dots are the pumping wells. Green dots are the installed monitor wells. ... 7	
Figure 2: Bar plot of monthly potential evapotranspiration and precipitation from 2012 to 2014 (based on RAWS climate station data)	8
Figure 3: Surface geology around research site (New Mexico Bureau of Geology and Mineral Resources, 2003, Geological Map of New Mexico, 1:500,000: New Mexico Bureau of Geology and Mineral Resources).....	9
Figure 4: Borehole logs of the 8 wells from Rio Grande (w8) to hill foot (w1) (Borehole logs data is from Miller, 2011)	10
Figure 5: Subsurface geology along Brown arroyo transect (SSP&A)	11
Figure 6: River stage and precipitation near research site from 2010 to 2014 (USGS) ...	12
Figure 7: Discharge difference (Escondida discharge minus San Antonio discharge) from Escondida to San Antonio stations (USGS).....	12
Figure 8: Consumptive use from San Acacia to San Marcial (M&I: Municipal and Industrial) (Shafike, 2004)	13
Figure 9: Pre-development groundwater table map within middle Rio Grande near the study site (Anderholm, 1987)	15
Figure 10: Comparison of river stage and groundwater fluctuations within the study area (USGS).....	16
Figure 11: The elevations of wells from survey and DEM.....	20
Figure 12: Structure of monitor wells and the water pressure logger. (Modified from Aaron Miller's report).....	21
Figure 13: A. The illustration of the slug test. B. Schematic illustration of Hvorslev analysis.....	23

Figure 14: R(t) values used in the one dimensional numerical model. It is the balance between the evapotranspiration and precipitation, recharge occurs when precipitation is larger than evapotranspiration calculated using the Kimberly-Penman equation, discharge occurs when evapotranspiration is larger than the precipitation.....	28
Figure 15: Boundaries and layers of the research site (The depth has been exaggerated by 20, different colors represents different water table elevations).....	32
Figure 16: The river stage during the specific period used for the specific storage analysis.....	37
Figure 17: Inverse correlation between barometric pressure change and water table fluctuations in wells, w3, w4 and w5.....	38
Figure 18: Homogenized slug test measurements in three wells	40
Figure 19: Normalized Difference Vegetation Index images in each month (The selected areas as high ET zones are enclosed in the polygons in image. 05/21/2013. They are consistent in images of other months.)	42
Figure 20: Numerical model in MATLAB loosely based on Rorabaugh's equation	46
Figure 21: Effect of river stage on simulated groundwater tables by dropping 0.5m	47
Figure 22: Effect of hydraulic diffusivity on groundwater tables by decreasing/increasing by 10 times.....	48
Figure 23: Effect of the magnitude of the source/sink term (R(t)) on simulated groundwater tables by decreasing/increasing 0.001m every day.....	49
Figure 24: Observed data versus best fit computed heads data from model calibration ..	52
Figure 25: Comparison of steady-state computed heads contour to published water-table map. (Orange: observed heads (Anderholm 1987), Blue: Computed heads (m) exported from MODFLOW model with interval 0.47m)	53
Figure 26: Comparison of observed and simulated groundwater table from transient MODFLOW model.....	56
Figure 27: Effect of change in river stage ($\pm 0.2\text{m}$) on simulated water table elevations .	58
Figure 28: Effect of change in riverbed conductivity on simulated water levels	59
Figure 29: Effect of change in drain conductivity ($\pm 2\text{m/d}$) on simulated water table elevations	60
Figure 30: Effects of pumping rate and the confining unit (Layer3) on water table elevations	61
Figure 31: Effects of evapotranspiration on groundwater table changes.....	62
Figure 32: Regional ET changes effects in the transient 3D model	63
Figure 33: Contour map of the steady-state 3D model with/without regional ET (Red area is the place where the groundwater tables are below the first layer (3 m), blue area is the place where the groundwater table is above the land surface.).....	64
Figure 34: Delineated wetland boundary based on 2013 data and the HSTS condition... Figure 35: (A) Comparison of the calculated steady-state flooded (Blue) and dry (Red) area with observed information; (B) (C) NDVI images of 09/26/2013 and 10/12/2013;	66

(D) Soil type, see Table 5-1 for soil properties description; (E) Wetland delineation based on transient model results, blue areas enclosed with black curves are the proposed wetland areas.....	68
---------------------------------------------------------------------------------------------------------------------------------------------------------------------------------------------------	----

LIST OF TABLES

Table 1: Locations of NRCS monitor wells on the wetland side of the study site, distances between wells and their available data period. (NAD_1983_UTM_Zone_13N)	6
Table 2: Precipitation, temperature and PET averaged for each month from 2012 to 2014 (RAWS)	8
Table 3: Well construction information of monitoring wells installed by the NRCS at the Bosquecito study site (See Figure 12 for graphical depiction of some of the variables used in Table 3). All units are in meters.	20
Table 4: Observed heads on four corners.	30
Table 5: Distance between stations and locations in the site	34
Table 6: Layer properties in research site	36
Table 7: Range of S_s in each well	39
Table 8: Parameters used in the specific storage calculation.....	39
Table 9: Hydraulic conductivity calculated in each well.....	41
Table 10: Colors in NDVI maps and their corresponsive NDVI ranges	42
Table 11: ET calculated in each month based on NDVI	43
Table 12: Days of different growing stages of chile. (From Brouwer & Heibloem, 1986).	43
Table 13: The crop coefficient for chili at different stages (From Brouwer & Heibloem, 1986).	43
Table 14: Interpolated days of each stage for chile in middle Rio Grande.....	44
Table 15: Calculated averaged evapotranspiration using Blaney-Criddle equation and its corresponding averaged pumping rate during growing season (p is from Blaney-Criddle, 1942, Table 1)	44
Table 16: Parameters used in the one-dimensional numerical model.....	45
Table 17: MODFLOW parameters and boundary conditions used in the steady state three-dimensional model.....	51
Table 18: Heads at each locations and their distances	54
Table 19: Observed and simulated hydraulic gradients on two directions	54
Table 20: Flow budget of the steady-state model	55
Table 21: Flow budget of the transient model	57

Table 22: Soil distributions and properties (Soil data is from NRCS SSURGO dataset). 69



This thesis is accepted on behalf of the faculty
of the Institute by the following committee:

Mark Person

Academic Advisor

Mark Person

Research Advisor

Fred Phillips

Committee Member

Jan Hendrickx

Committee Member

Daniel Cadol

Committee Member

I release this document to New Mexico Institute of Mining and Technology

Junhao Hu

07/22/2015

Student Signature

Date

CHAPTER 1

INTRODUCTION

1.1 Motivation

A wetland is considered to be a region where groundwater/surface water is at or near the land surface for much of the year. These regions are typically situated adjacent to surface water bodies in area of gentle topography. There are many definitions for wetlands from different state and federal agencies based on different purposes and criteria. The state of New Mexico defines a wetland as an area that is frequently inundated by surface or ground water such that can support aquatic/wetland vegetation typically adapted for life in saturated soil conditions (New Mexico Administrative Code).

Wetlands have some of the most valuable and diverse ecosystems in western United States (New Mexico Environment Department Surface Water Quality Bureau Wetlands Program, 2012). In New Mexico, only 0.6% of land area is classified as wetlands, but it accommodated up to 85% of all species that live in this area during a period of their life span (New Mexico Environment Department Surface Water Quality Bureau Wetlands Program, 2012). Wetland ecosystems are under threat in the western USA due to dam and draining ditches constructions, irrigation activities that may alter groundwater levels in the wetland area. Understanding the status of wetland becomes an essential work to protect the wild habitants-diverse area in New Mexico. Wetland delineation is one way to monitor the wetland status.

1.2 Methods of Wetland Delineation

A variety of methods are used in wetland delineation: hydric soil delineation method, hydrophytes survey, hydrograph analysis, topographic maps and aerial photography analysis are the most common ones.

Hydric soils are an important indicator of wetland. They have many unique features. Depletion of Fe/Mn is a common indicator of hydric soil. Reduced forms of Fe/Mn are highly mobile. When reduced, the Fe^{3+} and Mn^{4+} ions can be leached from the soil particles typically, leaving the sediment a neutral gray color. In addition, in the hydric soil region, organic matter accumulates because of anaerobic conditions in the

wetland. The organic matters often accumulates and results in a thick organic horizon, such as peat or muck, or dark organic-rich mineral surface layers and etc. (Vasilas et al, 2010). Finally, a ‘rotten egg’ odor is also a characteristic indicator of hydric soils which due to the accumulation of organic matter and the anaerobic conditions lead to emission of hydrogen sulfide gas. In some situations, not all of these indicators are present in hydric soils.

Hydrophytes are also wetland indicator. These could include cattails, saltgrass and coyote willow. These species of plants are well suited to the anaerobic condition of wetlands (Lyon & Lyon, 2011). Often if the wetland-thriving plants take more than 50% of the species in an area, the area could be categorized as wetland (Lyon & Lyon, 2011).

Hydrology is another way to delineate the wetlands. Indicators of wetland hydrology include recorded data on flooding and seasonal high (>1 foot depth) water tables, water marks on trees, drift lines, sediment deposits and drainage patterns as evidence of surface water flow (Majumdar et al, 1989). Specifically, areas where the groundwater stays continuously within one foot of the land surface for 14 days or the regions where the flooding happens during the growing season, repeated more than half of the years observed is believed to be the potential wetland area (U.S. Army Corps of Engineers, 2005).

US Geological Survey (USGS) large-scale topographic maps provide another way to roughly delineate the wetland. The potential wetland areas are typically within the topographic low lying areas or adjacent to surface water bodies. Combined with vegetation, land cover maps, etc. these provide a way to delineate a wetland or provide confirmation.

The aerial photos and remote-sensing image data are also very useful in the wetland delineation. In the visible and infrared portion of the electromagnetic radiation spectrum, the wetland has a very distinct reflectance shown in the aerial photo (Lyon & Lyon, 2011). Water-saturated wetland where inundation constantly remains, soils in wetland also have distinctive reflectance (Lyon & Lyon, 2011). Aerial photographs collected over long time period can be used to determine the dewatering or inundation of wetlands. Aerial photos provide an effective way to categorize wetland type according to given classification scheme, such as riparian wetland, bog or marsh.

Clearly, there are a lot of methods that can be used in wetland delineation. Every method has shortcomings. Usually, in wetland delineation, a combination of methods should be used according to the objective (Lyon & Lyon, 2011).

In this research, both field method, including the groundwater-table measurements, hydrograph analysis, and mathematical modeling are used to delineate the wetland. Automatic pressure transducers/data loggers were deployed in a series of eight wells in order to monitor the groundwater table elevations. The eight wells were installed starting near the Rio Grande bank to the foot of the uplands to the east. Based on the pressure data, and a series of slug test, the aquifer properties were estimated from the field data. All of this data was used to construct one-dimensional and three-dimensional groundwater flow models. Combined with the criteria that the groundwater tables must

maintain a depth of 1ft to the land surface for 14 consecutive days during the growing season, the groundwater table models helped delineate the wetland.

1.3 Study Objectives

The main goal of this research is to determine whether or not the hydrological modeling can provide a reliable wetland delineation map that is consistent with the results from field methods, such as hydric soil delineation. A secondary goal of this research is to understand what factors impact the water-level fluctuations within this wetland. We considered the effects of river stage, riverbed conductivity, drainage systems, evapotranspiration, groundwater pumping/irrigation and layer properties. The modeling results provide valuable information for wetland protection in this semiarid region.

1.4 Prior Hydrological Modeling Studies on Wetlands

A number of numerical models having varying levels of complexity have been used to study the hydrology of wetlands. These models have been used to quantify groundwater or surface-water flux recharging wetland, ponded-water depth fluctuations, nutrient transport prediction, and wetland restoration design. These models can be categorized as models for surface-water flow, models for groundwater flow and models of surface-water groundwater interactions.

Feng et al (2013) used SWAT, a spatially-distributed hydrological modeling system with a wetland module to quantify the hydrologic condition within the Zhalong wetland located in northeast China. They tried to determine what were the influential factors controlling surface water discharge from the wetland, as well as ponded-water depth in order to assess the wetland's ecosystem health (Zhang et al, 2005). Monthly streamflow data was used to calibrate and validate the model. Results revealed the importance of the upstream river basin drainage area on the wetlands function. Obropta et al (2008) used the USEPA SWMM model to predict the surface-water movement through a reestablished urban wetland area of Teaneck Creek, New Jersey. In this model, groundwater flow, vegetation and soil data were considered. Individual rainfall events were incorporated into this model, and surface water flow was calculated. The calculated flow data was compared to observed surface-water discharge data in the model calibration exercise. Later, a monthly water budget for this wetland was calculated.

Alaghmand et al, (2014) considered the impacts of river stage on the salinity of floodplain groundwater in Australia using HydroGeoSphere. Flow and nutrient transport were coupled and calibrated against the groundwater tables at wells and the concentrations of solutes from observation well data. The results demonstrated that the river bank storage determined the interaction of groundwater and surface water and controlled the salinity of the river-bank riparian system. The river stage was found to be the main controlling factor for the bank storage. Gerla (1999) considered the role of groundwater in wetland function using modeling method and DEM. He considered two study areas located in Williams and Mary Lakes area and the Shingobee River in north-central Minnesota. He showed that the groundwater tables had a similar pattern with the land surface elevation (Toth, 1963). This method provided estimated information of the

potential groundwater recharge and discharge within a watershed under its various assumptions. Joris and Feyen (2003) modeled the fluid flow and soil-moisture redistribution along a transect in a fluvial groundwater-fed wetland located in the middle reach of river Dijle in Belgium, using HYDRUS2D. These authors showed the seasonal variations in soil moisture along the transect as well as groundwater levels. Karan et al, (2013) used a variety of field methods, such as the electrical resistivity tomography to detect the geological heterogeneity of a wetland located in Holtum Stream in Denmark. Groundwater fluxes were derived from streambed temperature, sampling and analysis of the geochemistry. These authors developed a three dimensional groundwater model using MODFLOW; they assessed the controlling factors on nutrient loading in wetlands and streams in this study area.

Kazezyilmaz-Alhan et al, (2007) discussed about the hydrology and water quality in a restored wetland located in Duke University that was influenced by groundwater and surface water interactions. They developed a general comprehensive dynamic wetland model (WETSAND) that was linked to a surface-water model in SWMM5 for an upstream urban area, considering both water quantity and water quality in the Duke University restored wetland. This model proved that the surface water and groundwater interaction was generally very important in wetland controlling function. Krause & Bronstert (2005) investigated the interaction between the river and the flood plain zone, which they referred to the ‘Direct Catchment’, by using the model IWAN which is a combination of the deterministic distributed hydrological model WASIM-ETH and the numerical groundwater model MODFLOW. WASIM-ETH can represent runoff and unsaturated soil moisture redistribution. The MODFLOW component of this code represented groundwater and its interactions with the surface water. The delineation of the ‘Direct Catchment’ was done with the combination of the field observations and modeling results. Also, this model tested the dynamics of groundwater recharge and discharge. Hattermann et al; (2006) studied the integration of the wetland and the riparian zone using SWIM (Soil and Water Integrated Model) which was based on the SWAT and MATSALU hydrologic models. They assessed the impacts from wetlands on the water balance and nutrient balance of the river basin.

Most of the above mentioned studies have focused on using hydrologic models to quantify water and nutrient budgets in wetlands. There are very few studies that have focused on using hydrologic models in wetland delineation. One notable exception was the study of Boswell & Olyphant (2006) who developed a saturated-unsaturated groundwater flow model for the Lake Station Wetland Restoration site in Lake County, Indiana. Combined with various field data, such as soil water tension, saturated hydraulic conductivity, precipitation and potential evapotranspiration, these authors calibrated their model against observed hydraulic head data. They used their calibrated model to assess temporal and spatial variation of the wetland hydroperiod (ponded period) in this field.

CHAPTER 2

STUDY AREA

2.1 Location

The Bosquecito wetland is located in the upper riparian region of Bosque del Apache, approximately 6.52km south of Socorro and 9.18km north of San Antonio, New Mexico, USA, on the east side of the Rio Grande (Figure 1A). The northern boundary of the study area stopped at the Arroyo de la Canas (Figure 1B). The southern boundary is located approximately 4 km south of the north boundary. The western boundary is at the end of the agricultural fields to the west of the Rio Grande. The eastern boundary is along the Bosquecito road at the foot of the remnant upland. The study area has a length from west to east of 2698 m, and a length from north to south of 3887 m. It has an area of about 9.4 km^2 , which includes the western irrigation land and the eastern wetland site (Figure 1B). The land surface rises rapidly to the east of the study area. We assumed that recharge to the east was negligible. This assumption requires further investigation to confirm. The eastern part of study area used to be farmed during the early-to-middle 1900's. The topography of the area is relatively flat, with a topographic gradient of -6.4E-5 from east to west direction and 1.0E-3 in the north to south direction. An abandoned irrigation ditch running N-S is one of the topographic high features to the east of the Rio Grande, in the wetland area.

The National Resources Conservation Service (NRCS) has used this wetland as a research site since 2010. A series of 10 wells were installed and water-level data has been continuously collected from 2010 to 2014 (Table 1). Well w8 is the well nearest to the Rio Grande. Its hydrograph is strongly affected by the river stage. Well w1 is the furthest from the river, and closest to the east boundary of the study area (Figure 1A). The average distance between the wells is 206m. At well w4, two additional monitoring wells were installed, one to the north and south side respectively in order to determine the north-south hydraulic gradient. These are spaced about 50 m from well w4. HOBO pressure transducers were installed in wells w1 to w8. The HOBO transducers recorded water pressure head hourly. Barometric pressure is also measured at well w4. (Figure 1B). All the pressure data in each well was converted to groundwater table elevation for this study. The groundwater table was also manually measured by using the Solinst water level meter every two weeks.

At well w4, which is the middle of the research site, a weather station was installed to record the solar radiation, wind speed, wind direction, air temperature and precipitation. However, because of a malfunction of the weather station in the middle of the research period, we used climate data from the RAWS station situated in Bosque del Apache which is approximately 24 km south from the research site, and at an elevation 37m lower.

ID	W1	W2	W3	W4	W5	W6	W7	W8	S04	N04
Easting m	328653	328582	328482	328238	327971	327723	327385	327269	328249	328265
Northing m	3763922	3763958	3764000	3764093	3764148	3764173	3764172	3764269	3764026	3764161
Distance between wells m	78.1	113.9	257.7	270.9	248.7	339.9	132.6			
Record Periods				7/2010 to 7/2014					06/2013 to 07/2014	

Table 1: Locations of NRCS monitor wells on the wetland side of the study site, distances between wells and their available data period. (NAD_1983_UTM_Zone_13N)

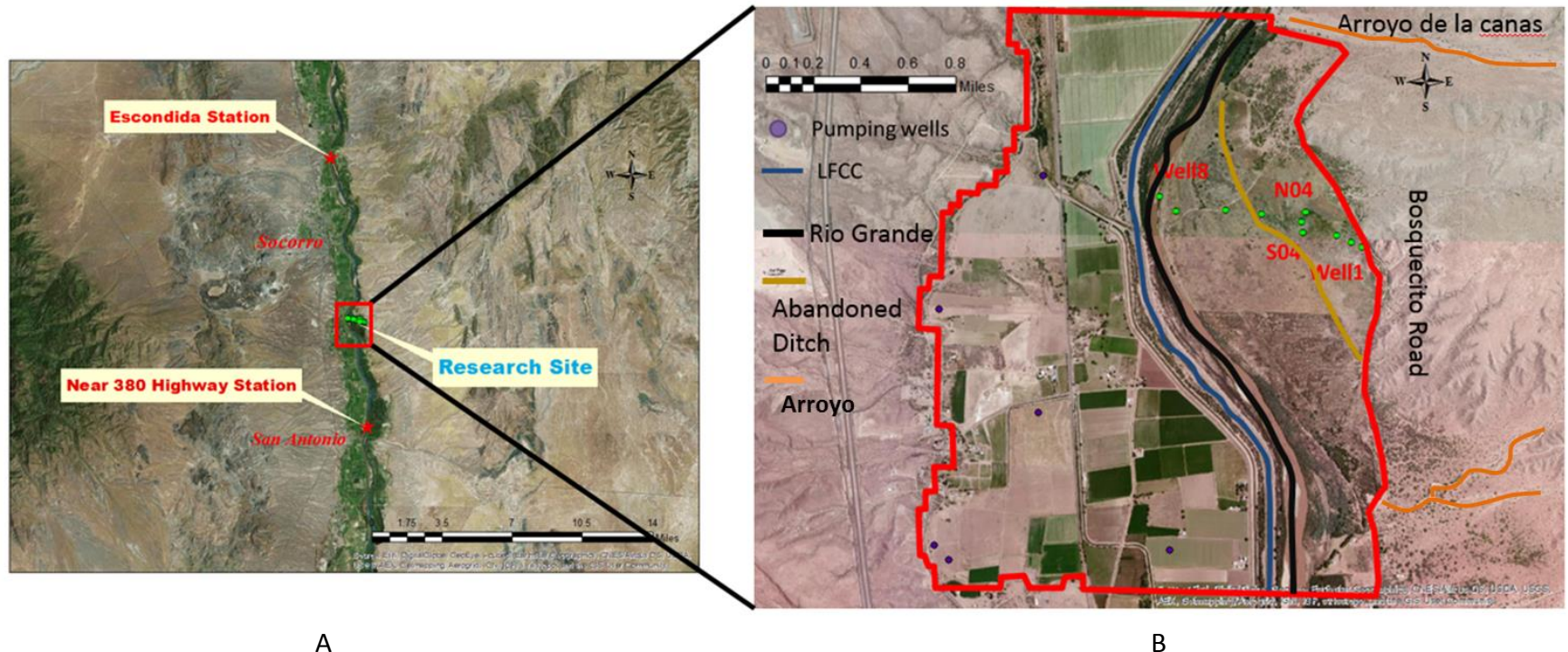


Figure 1: A. Location of the research site along the Rio Grande near San Antonio, NM. The green dots denote the locations of 10 monitoring wells installed as part of this project. The red stars denote the locations of stream gauge stations along the Rio Grande. B. Boundary of the research site and 3D model domain (thick red line). The low flow conveyance channel (LFCC) is denoted by light blue line. The Rio Grande in the research domain is the black line. Yellow line is the abandoned ditch. Orange lines stand for the arroyos. Purple dots are the pumping wells. Green dots are the installed monitor wells.

2.2 Climate

Precipitation at this site ranges from 0.2 mm/d. to 1.3 mm/d. on average, and the mean annual precipitation averages 2 cm. Temperature in this site ranges from -5 °C to 34 °C, and annual average temperature is 14 °C. Bosquecito has a semiarid climate type. Potential ET (Kimberly Penman) exceeds precipitation. Large precipitation events occur from July to September during the monsoon season (Figure 2). There can also be large fall precipitation events from the Gulf of Mexico as hurricanes moves through. The coldest months are in December and January. The highest temperatures occur between May and August (Table 2). March to November is the irrigation season in New Mexico.



Figure 2: Bar plot of monthly potential evapotranspiration and precipitation from 2012 to 2014 (based on RAWS climate station data)

Month	Precipitation mm/d	Temperature °C	PET mm/d
Jan	1.7×10^{-1}	2	2.5
Feb	3.4×10^{-2}	6	3.4
Mar	6.8×10^{-2}	11	4.5
Apr	1.6×10^{-1}	16	5.1
May	1.9×10^{-1}	19	5.6
Jun	8.5×10^{-2}	26	6.4
Jul	1.8	26	4.6
Aug	1.6	21	4.0
Sep	2.9	16	3.5
Oct	3.5×10^{-1}	13	4.1
Nov	1.7×10^{-1}	6	3.2
Dec	3.5×10^{-1}	3	2.6

Table 2: Precipitation, temperature and PET averaged for each month from 2012 to 2014 (RAWS)

2.3 Geology

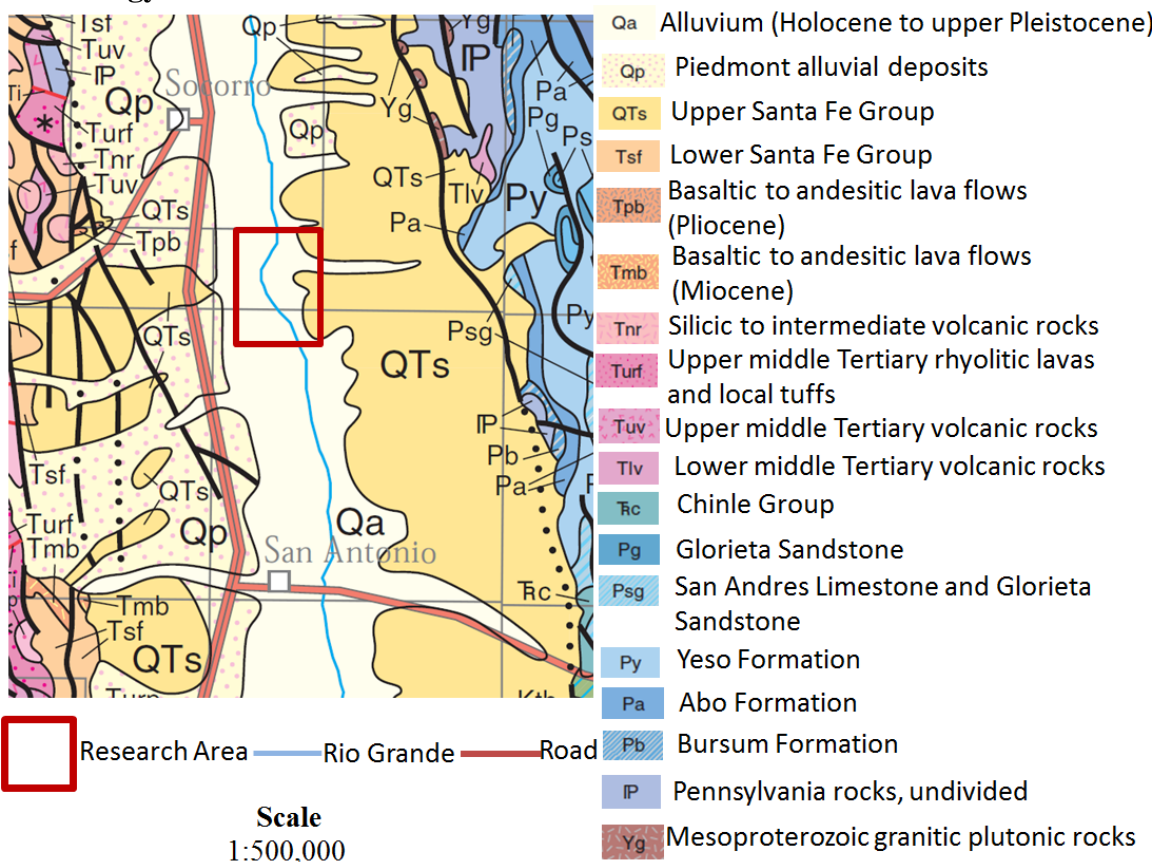


Figure 3: Surface geology around research site (New Mexico Bureau of Geology and Mineral Resources, 2003, Geological Map of New Mexico, 1:500,000: New Mexico Bureau of Geology and Mineral Resources)

Surficial sediments at this site mostly consisted of alluvium (Sands and silt) (Figure 3). Because of its relatively low topography and shallow water table, slowly decaying organic matter remains in the region from well w5 to w1. The surface soil at these wells has a thick layer of silty clay or fine sand rich in organic matter (Figure 4). In the region from wells w8 to w6 which has higher topography and deeper water tables, less organic matters occur, and the matrix texture is coarser with a relatively higher permeability.

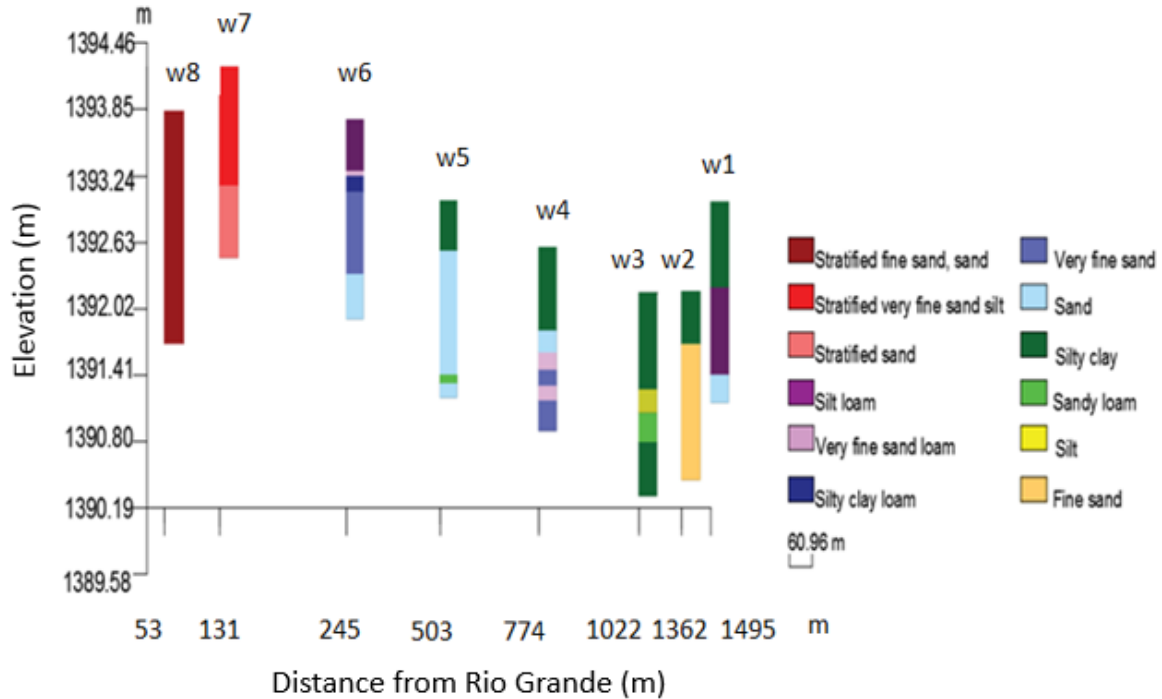


Figure 4: Borehole logs of the 8 wells from Rio Grande (w8) to hill foot (w1) (Borehole logs data is from Miller, 2011)

Additional geologic constraints are available from prior studies. Along Brown arroyo, which runs across the research site, 11 wells were installed by S.S.Papadopoulos & Associates, Inc. in 2003 (Figure 4-7, Wilcox, 2003). These wells were used in an aquifer test. They were also formerly used as groundwater monitoring wells. The well logs provided a good source of information on the subsurface geology (Figure 5). The deepest of these 11 wells has a depth of 25.3 m. The shallowest well is 15.2 m deep. The hydrogeology of the study area can be categorized as a four-layer system. The first layer is 3 m thick and consists of silt and clay, second layer is 6 m thick and is composed of sand. The third layer is a confining layer 1m thick with silt and clay again. The fourth layer starts from a depth of 10 m with sand and gravel. Bed rock lies under the base of layer 4. More organic matters accumulation increases with distance from the river in layer 1, hence the hydraulic conductivity is lower, while the hydraulic conductivity near

the river is higher (Wilcox, 2003).

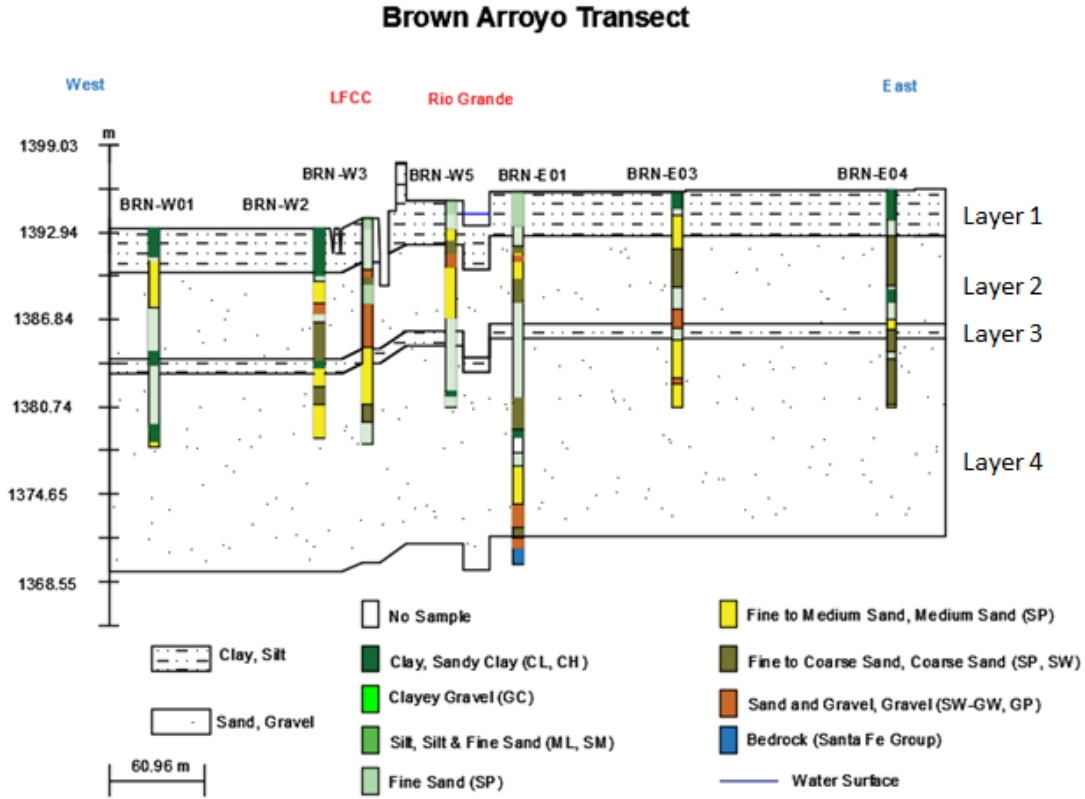


Figure 5: Subsurface geology along Brown arroyo transect (SSP&A)

2.4 Hydrology

2.4.1 Rio Grande Stage/Discharge

The Rio Grande sources and originates in southern Colorado, within the San Luis Basin. Snow melt is the main source of Rio Grande water (Rango, 2006). The river flows through the center of the study area. River stage for this site is interpolated linearly from the two gauge stations nearest to this site to the north and south, based on the distance to the site. To the north, the gauge station is approximately 12 km away from the site. To the south, the station is 6 km from the study area (Figure 1A). From June to November, the Rio Grande is sometimes dry in this section; flow returns following monsoon precipitation events. The river stage usually peaks during November to March. (Figure 6)

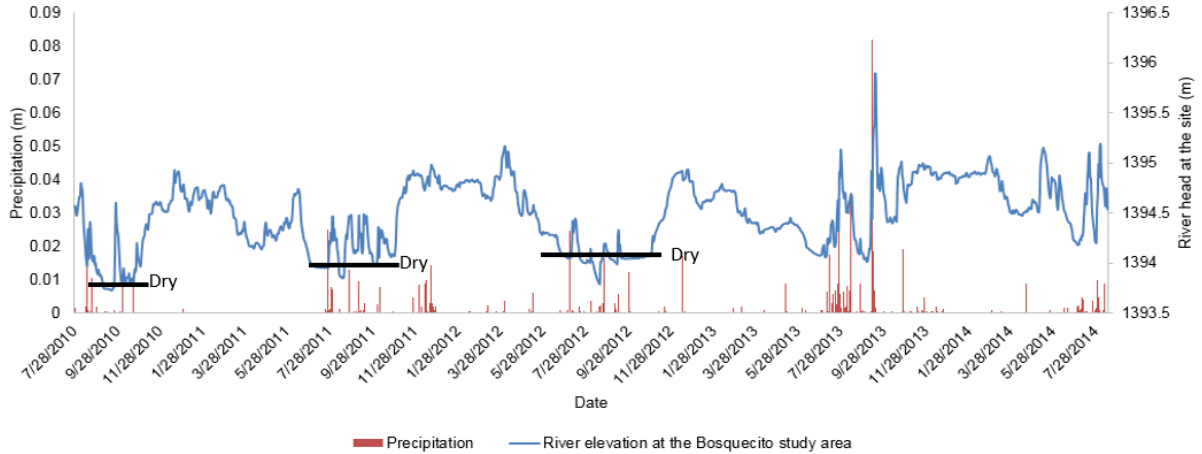


Figure 6: River stage and precipitation near research site from 2010 to 2014 (USGS)

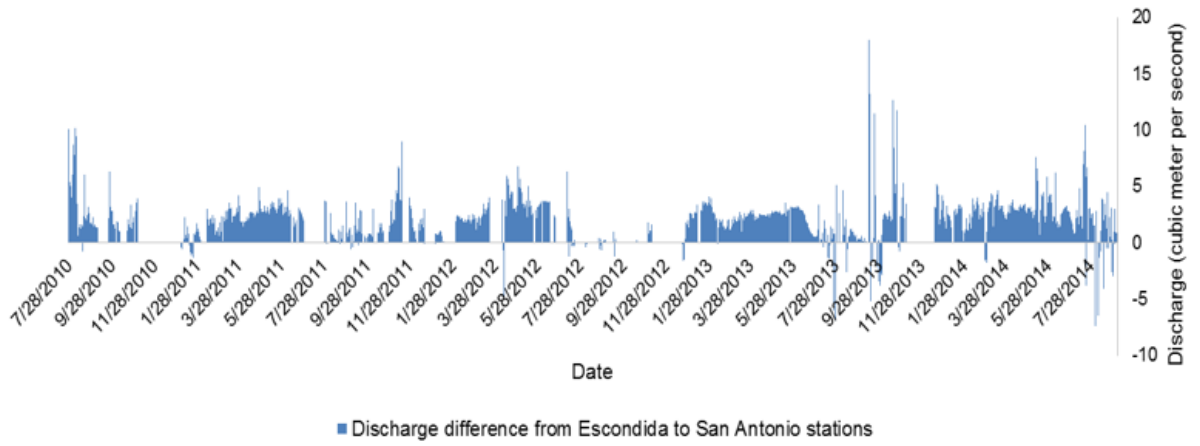


Figure 7: Discharge difference (Escondida discharge minus San Antonio discharge) from Escondida to San Antonio stations (USGS)

On average, the Rio Grande loses water at the section from Escondida to San Antonio (Figure 7) which runs through the research site from north to south. Riparian evapotranspiration, crop evapotranspiration, open-water evaporation, municipal and industrial consumption, and groundwater outflow all contribute to reduction in stream flow between Escondida and San Antonio, NM (Figure 8). Most of the river water goes to the riparian ET. Crop evapotranspiration is the second biggest use of Rio Grande water. The vegetation transpiration along the riparian corridor of the Rio Grande (which includes the wetland areas) also consumes a big portion of Rio Grande water. Open-water evaporation consumes about 8% of the river water. Municipal and industrial (M&I) consumption is about 1% of Rio Grande discharge (Figure 8) (Shafike, 2004).

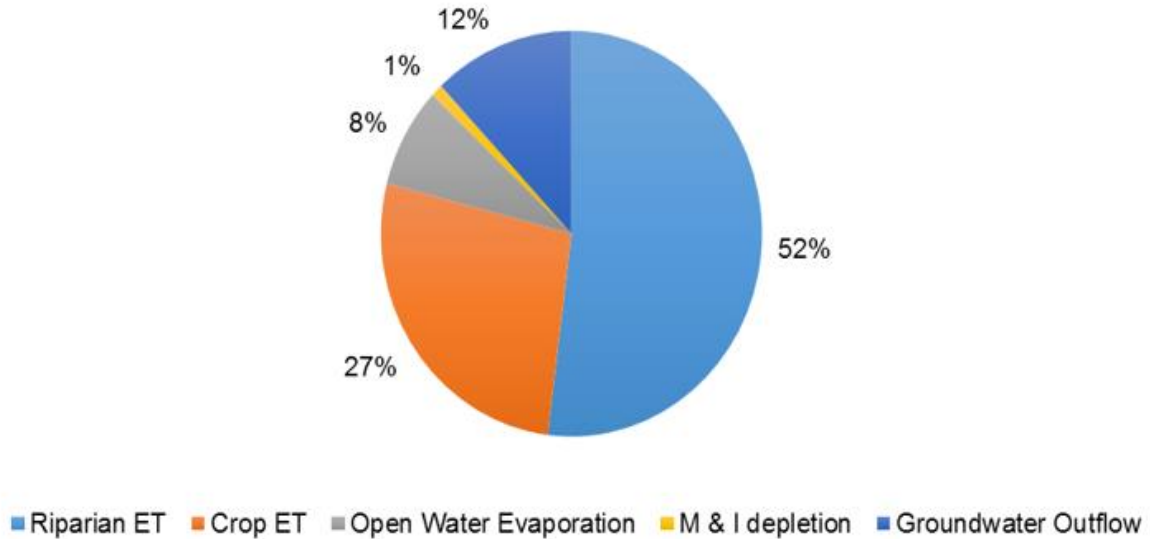


Figure 8: Consumptive use from San Acacia to San Marcial (M&I: Municipal and Industrial) (Shafike, 2004)

2.4.2 Riverbed Conductance

The riverbed conductance was estimated by means of a sulfur hexafluoride (SF_6) tracer test; conducted along the Escondida transect (Cardenas 2006). Cardenas (2006) installed four piezometers drilled along this transect. One was used for injecting dye SF_6 , the other three were used to monitor the dye flux peak. The injection well had a screen at the shallowest depth at 0.5 m; the other three respectively had screen depths of 0.9m, 1.2m, 1.5m. The monitor wells were sampled before the dye release in order to have a background concentration of SF_6 . After the dye release, the water in the monitor wells was sampled in a time interval ranging from 2 to 3.5 hours at beginning. The time interval became longer when the concentration of the dye reached the tailing period. Only the samples of the injection well and its nearest monitor well were delivered to and analyzed at the University of California at Santa Barbara. The head difference between the injection well and the nearest monitor well was manually measured as 1 to 2 cm. Based on the breakthrough curve and Darcy's law, the vertical hydraulic conductivity was calculated to be between 6.4 m/d and 12.8 m/d. (Cardenas, 2006)

2.4.3 Low Flow Conveyance Channel

The low-flow conveyance channel (LFCC) was constructed during the 1950s to provide conveyance of water to Elephant Butte reservoir near Truth or Consequences, NM. From 1959 to 1986, it was very actively functional. Currently, it has not been used for flow diversion, otherwise it functions passively as the main drain along the river corridor (Shafike, 2004). The LFCC is located to the west of the Rio Grande at the study site (Figure 1B). During period of flooding, excessive water from Rio Grande is diverted

to the LFCC (Gorbach, 1999). As discussed later, the LFCC affects the groundwater tables in the wetland side by changing the Rio Grande stage.

2.4.4 Agriculture Canals and Drains

Numerous drains and ditches for irrigation have been constructed along the Rio Grande in and around the study site. The longest one in this study domain is the Socorro main irrigation canal. Many other shorter canals, such as the Luis Lopez drain, McAllister Drain, etc., are also connected to the Socorro main canal. The Socorro main canal is designed to be deeper than the connected irrigation ditches, so the excess water from irrigation will run into the canal and be drained to the Rio Grande.

2.4.5 Arroyos

There are several arroyos around the research site that could deliver storm runoff to the study area (Figure 1B). Most of the time, the arroyos are dry. During the monsoon season, large precipitation events; result in storm runoff flooding the otherwise dry arroyos within the research site, causing the water tables to rise.

2.4.6 Groundwater Table Elevations

Groundwater within this region was studied by Anderholm in 1987. More recent studies including Shafike (2004) and Wilcox (2003) provide additional work on hydrology investigation along Rio Grande, such as river water consumption and groundwater modeling in a large scale.

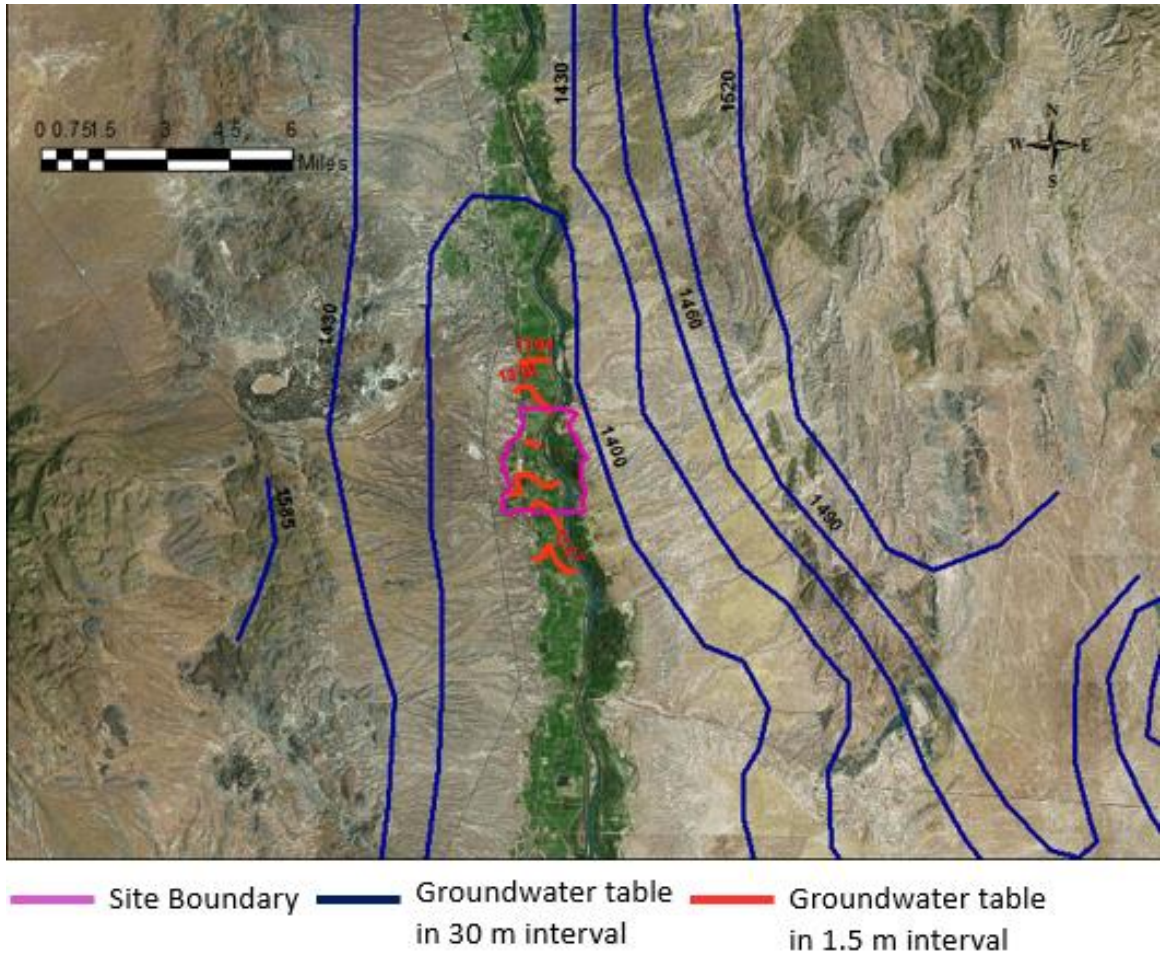


Figure 9: Pre-development groundwater table map within middle Rio Grande near the study site (Anderholm, 1987)

Anderholm (1987) presented pre-development water-table elevation maps using both 30 m and 1.5 m contour intervals (Figure 9). Regional water-table contours suggest there might be some recharge to the site from the east and west sides (Figure 9). To the east of the study domain within the upland area, the water table is high and water table gradients are primarily oriented in an east-to-west direction. To the west, the water-table gradient is primarily west-east. However, along the Rio Grande corridor, the observed groundwater table gradient is primarily oriented in a north-south direction (Figure 9, Orange lines).

In the field, groundwater table fluctuates with an amplitude of about 1-3 m (Figure 10). Many factors influence the groundwater elevation fluctuations. These include surface-water groundwater interaction, precipitation/recharge, evapotranspiration, the LFCC, irrigation and pumping on the west side of the study domain. Precipitation and the irrigation water to the fields on the west side of the study area are all potential recharge sources. Evapotranspiration, groundwater pumping to the west of the site are the

groundwater sinks. River stage is an important factor that controls the groundwater fluctuation patterns in the research site (Rorabaugh, 1964) (Figure 10).

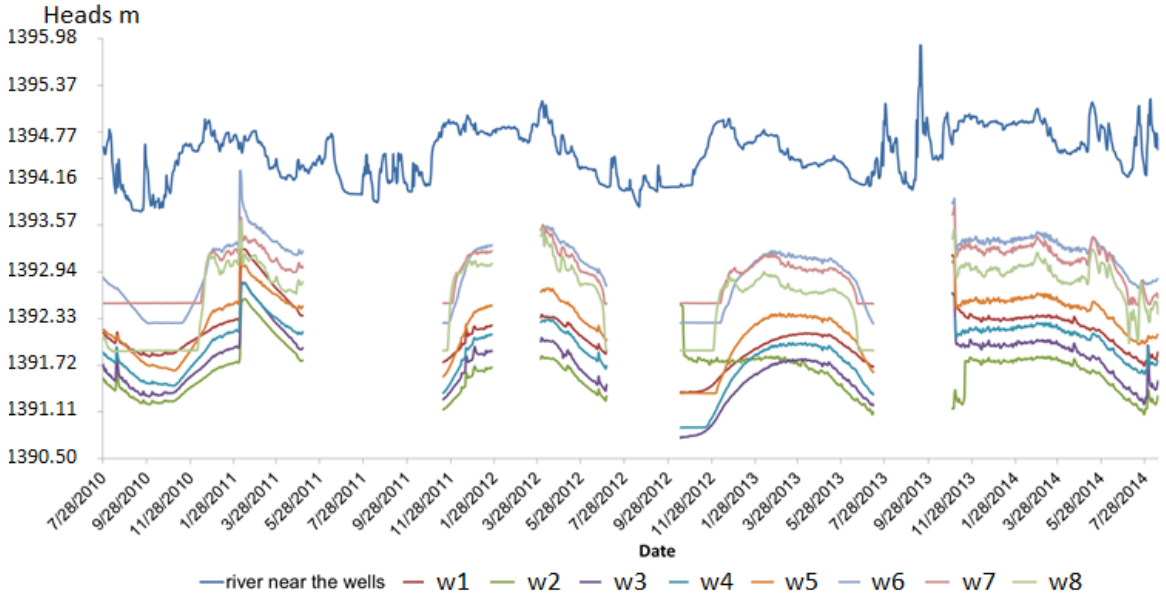


Figure 10: Comparison of river stage and groundwater fluctuations within the study area (USGS)

2.4.7 Aquifer Tests

An aquifer pumping test was performed by S.S.Papadopoulos & Associates, Inc. (SSP&A) in 2003; to measure the hydrologic properties of the aquifers along the Rio Grande (Richard, 2006). The pumping test was performed along the San Acacia reach of the Rio Grande near Highway 380 transect. (Richards, 2006). Both analytical solutions and numerical models were used to estimate aquifer parameters.

There were 14 wells installed for this pumping test. The production well was located 67 m west to the Rio Grande and 58 m east to LFCC. (Richard, 2006). The rest of the wells were used as observation wells located around the extracting wells. All these wells were scattered on the west side of Rio Grande. The pumping well had a screen at depth around 11 m to 18 m with a diameter of 254 mm. The monitoring wells were screened at depths of 26 m to 28 m. In addition, 6 monitoring wells were screened in the shallow aquifer; the other 6 wells' screen has a similar depth as the extracting well's screen depth. The result showed that the deepest well and the medium-depth wells reach stabilization in about 10 min, which is a very fast response to the pumping well. The shallow aquifer wells located above the confining unit (hydrostratigraphic layer3) did not stabilize during the test, and the water table change was very small.

After the aquifer test, two analytical methods were used to calculate the layer properties in this site, two numerical analysis were also conducted to further study the test. Based on the test, analysis and calculations, Richards (2006) concluded that a low-permeability confining clay layer exists at a depth of about 9 m. The horizontal and

vertical hydraulic conductivities for the upper phreatic aquifer were estimated to be 20.6 m/d and 1.33 m/d respectively. The horizontal and vertical hydraulic conductivities within the lower leaky-confined aquifer were estimated to be between 45.7 m/d and 20.6 m/d respectively. Hydraulic conductivity for the middle confining unit was not determined in the test.

2.5 Vegetation

The vegetation within the Bosquecito wetland at the study site is very diverse, such as Cattail, Inland Saltgrass, Annual Sunflower, Coyote Willow and Russian Olive, etc (Aaron Miller, 2011). Plant species in a wetland are determined by many factors. Different types of wetlands may have different vegetation. The salinity of water, the drainage ability, soil type, temperature and the precipitation can influence the wetland vegetation. It is said that the Rio Grande supports one of the most diverse and thriving riparian forests in the Southwest United States (Hink and Ohmart 1984). In order of areal coverage, the typical wetland plants in Bosque del Apache area are Coyote willow, Saltcedar, Gooddings willow and Cottonwood. (Siegle et al, 2010).

2.6 Fauna

This site provides a habitat for many kinds of reptiles, amphibians, insects, birds, fish, and mammals, such as northern leopard frog, Canada goose, sand hill cranes and Rio Grande silvery minnow. It is a natural nursery for animals to thrive, this includes the animals only found in wetland area.

2.7 Previous Hydrological Modeling Studies

Groundwater numerical modeling studies on Rio Grande basin had been done by many researchers. Shafike (2004), Wilcox (2003) and Richard (2006) all developed hydrologic models for the middle Rio Grande which includes this site. Their models were in large scale covering the entire Socorro/La Jencia basin. Shafike and Wilcox's field work and models provided some basic geological and aquifer properties used in this study. Richards developed her model based their former work, but specifically had a discussion on the effect of the low-permeability layer underneath her study area in her model.

In this study, we used some of the geological data and aquifer properties from prior studies. We first developed a one-dimensional numerical model loosely based on Rorabaugh's equation testing the influence of river stage on water table fluctuations. This was built in MATLAB. Next, we constructed a three-dimensional hydrogeologic model considering the river stage, river bed conductivity, geological layer properties, evapotranspiration and human impacts had been built in MODFLOW. The purpose of this model was to find out the most influential factors for the wetland groundwater fluctuation and delineate the wetland area. A sensitivity analysis was then performed using these models to find the most influential factors/parameters controlling the

groundwater table in the wetland side. The wetland area was delineated using the calibrated MODFLOW model.

CHAPTER 3

METHODS

3.1 Overview

This project combines the field investigations, hydrographs and data analysis, satellite image analysis and hydrological modeling approaches, using Excel, ArcGIS, AutoCAD, ERDAS, MATLAB and MODFLOW to assess the most influential factors controlling groundwater fluctuation within the Bosquecito wetlands and to use computed water-table depths to delineate the wetland area.

HOBO pressure transducers were installed in the 8 monitor wells and water-pressure measurements were recorded at every hour. Manual collection of water levels in the wells was done every two weeks between 07/2010 and 07/2014. Based on the recorded groundwater fluctuation data, specific storage S_s was estimated by hydrographs analysis. It was estimated for the upper confined aquifer using barometric pressure and water-level data (Spane, 2002). Barometric pressure and aquifer water levels were analyzed over a 56-day period. Slug tests were also performed at this site in November 2014, to measure the hydraulic conductivity of the shallow confined sands across the study area. Monthly potential evapotranspiration rates were estimated using the Blaney-Criddle method (Blaney & Criddle, 1949), while the yearly average potential ET was based on the Kimberly Penman method calculated from RAWS station (Dockter, 1994). These measurements and analysis supplemented hydrological data from prior regional studies that were used in the hydrologic models.

A one-dimensional numerical model loosely based on the approach first presented by Rorabaugh (1964) was developed in MATLAB. This analysis tested the influence of river stage fluctuation on the groundwater table variations within the study area. A three-dimensional numerical model of this site was also developed using MODFLOW. This model included many other hydrologic stresses and factors, including river bed conductivity, multiple hydrogeologic layer properties, evapotranspiration, regional drains including the LFCC and irrigation/pumping. A sensitivity analysis was performed in this site to determine the most influential factors for this site. The calibrated model also permitted us to determine the lateral extent of the wetland through analysis of what areas had the water table within one foot of the land surface for two weeks or more in more than half of the years considered.

3.2 Field Methods

3.2.1 Groundwater Table Fluctuation Monitoring

Groundwater table was recorded since 2010 by Dr. Aaron Miller of the National Resources Conservation Service every two weeks between July, 2010 and July, 2012 using a Solinst electric water level meter. A total of 8 monitor wells were installed in this site. Details of the well constructions are listed in Table 3. The wells were installed starting 53 m (W8) and extending to 1495 m (W1) east of the Rio Grande (i.e., between the bank of the Rio Grande channel and the base of the east remnant uplands). For the surveyed land surface elevations of the wells are based on an unknown datum, the survey elevations were shifted down based on w5, since w5 is located in an area where no tall plants reside. The elevations were adjusted by comparison of the DEM and survey data. W8 is elevated by 0.3 m, while w1 is lowered by 0.5 m (Figure 11). A HOBO pressure transducer recorded the water pressure and temperature data every hour. A schematic diagram depicting some of the variables listed in Table 3 is presented in Figure 12.

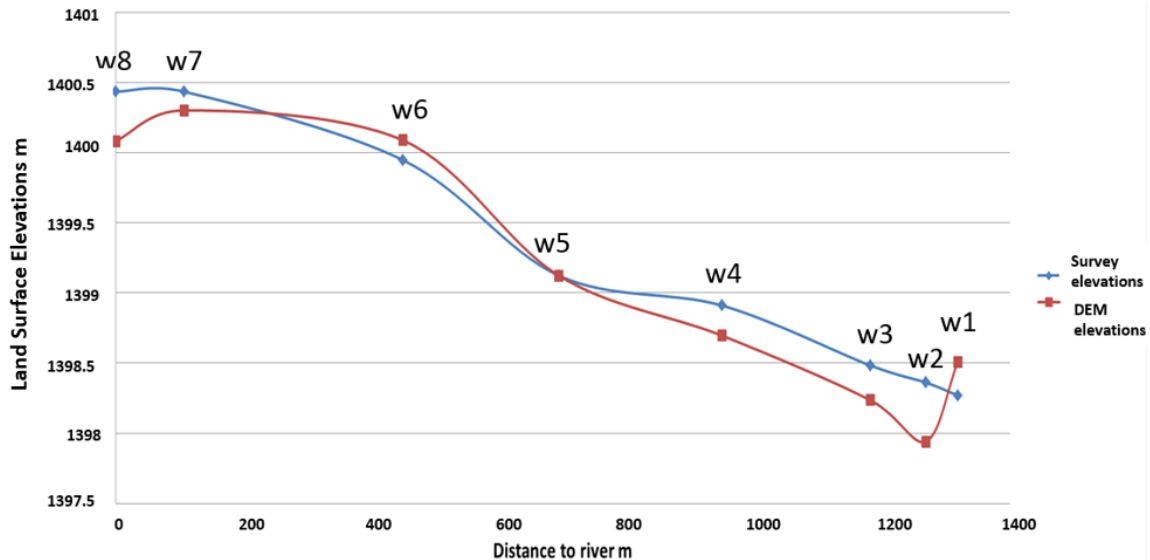


Figure 11: The elevations of wells from survey and DEM

Unit: m	w1	w2	w3	w4	w5	w6	w7	w8
Total length	1.83	1.65	1.75	1.68	1.80	1.83	1.75	2.13
Screen location	1.7	1.52	1.62	1.55	1.67	1.7	1.62	2
Well diameter	0.05	0.05	0.05	0.05	0.05	0.05	0.05	0.05
LS	1392.5	1392.2	1393.0	1392.2	1393.0	1392.2	1393.0	1392.5
D _t	2.16	2.16	2.16	2.16	2.16	2.16	2.16	2.74
H _i	0.62	0.38	0.43	0.40	0.42	0.38	0.42	0.60
Pressure Transducer type	HOBO pressure transducer							

Table 3: Well construction information of monitoring wells installed by the NRCS at the Bosquecito study site (See Figure 12 for graphical depiction of some of the variables used in Table 3). All units are in meters.

In well w4, a barometric HOBO pressure logger was installed above the water table. Both the water pressure readings in the wells and the barometric pressure readings were used in the groundwater table elevation calculation (3.1).

The water pressure recorded by the HOBO pressure transducer is the sum of the barometric pressure and the pressure from the water column above the pressure transducer. Based on the relationship between the water pressure and water depth, the pressure data was converted to water depth in wells using equation below:

$$D1 = \frac{P_i - P_b}{\rho g} \quad (3.1)$$

where P_i is the (pascal) water pressure above the HOBO transducer in well i; P_b is the (pascal) barometric pressure at the Bosquecito site located near well w4; ρ is the density of water (1000 kg/m^3); g is the gravity of earth (9.8 m/s^2); $D1$ is the depth (m) of water above the transducer.

Measurements were recorded hourly and the data was downloaded every 2-4 weeks. The water depth in the wells was converted to water table levels using the following equation:

$$WT = LS + Hi - L + D1 \quad (3.2)$$

where LS is the land surface elevation; Hi is the height of riser tube above soil surface; L is the length of transducer and its suspension cable; $D1$ is the depth (m) of water above the transducer; WT is the groundwater table elevations. (Figure 12; Table 3).

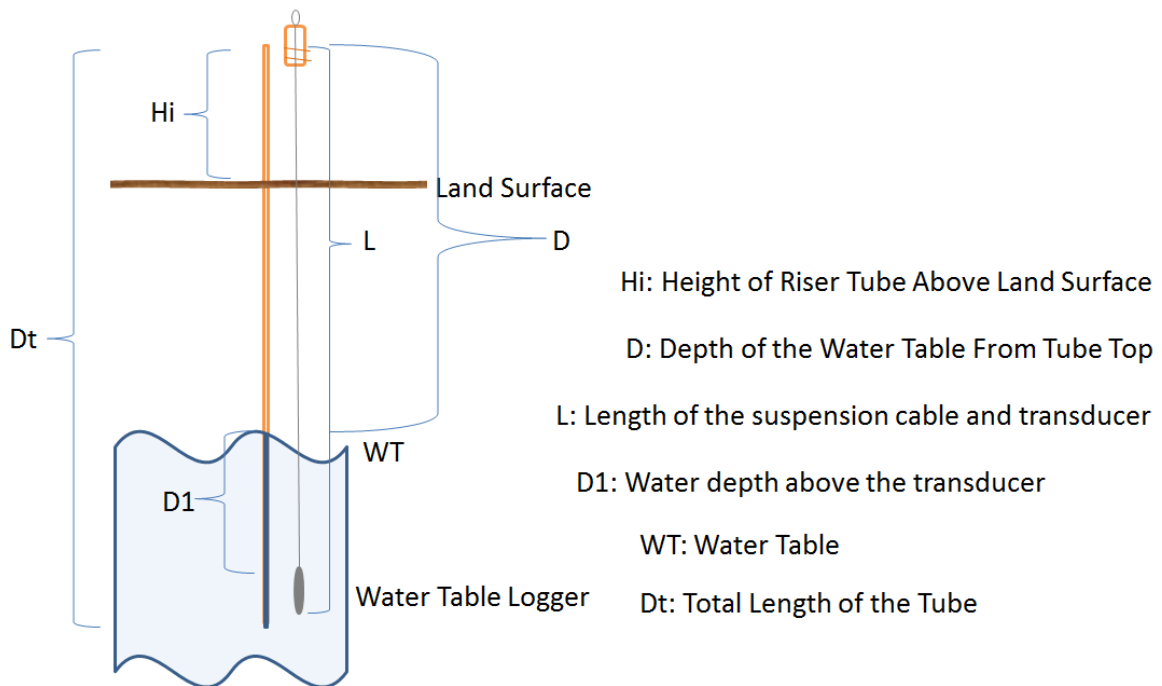


Figure 12: Structure of monitor wells and the water pressure logger. (Modified from Aaron Miller's report)

Because of equipment sensitivity and calculation, the automatically collected pressure data from the pressure transducers may result in some errors. In order to calibrate the automatically recorded data, manual water depth measurements were collected every two weeks using a Solinst Electrical Water Level Probe. The groundwater table level is calculated from water depth using this relationship:

$$WT = LS - (D - Hi) \quad (3.3)$$

where LS is the land surface elevation; D is the depth of water from tube top; Hi is the height of the riser tube above land surface; WT is the groundwater table elevations. (Figure 12; Table 3)

By comparison, the exact water table levels were calibrated. The calibrated logger data was later inserted in the models for the periods from 10/15/2012 to 07/12/2013 and from 10/31/2013 to 08/15/2014.

3.2.2 Hvorslev Slug Test

The uppermost permeable layer of the sediments within the research site is the focus of this study because it has the primary control on groundwater surface water interaction and determines the wetland delineation. It is very important to get a relatively reliable hydraulic conductivity measurement for this unit. On November 10th, 2014, slug tests (Figure 13A) were performed on these wells: w1, w2, and w3 (Figure 1B). These three wells, wells are situated furthest from the Rio Grande channel, nearest to the uplands. All these wells located area has a thick relating organic clay layer at the surface and the overlying fine sands are the finest (Figure 4). The slug test was performed with the following equipment: a solid slug with a diameter of 0.02m, 0.27m in length, an In-Situ Level TROLL 700 pressure transducer data logger, a Solinst Water Level Meter, an In-Situ Rugged Reader Handheld PC and duct tape (Figure 13A)

The slug test was performed according to the following steps: 1) The depths to water and the well bottom were measured in the well using the Solinst Water Level Meter to make sure that there was a thick enough water column in the well to immerse the pressure transducer. 2) The pressure transducer was set near the bottom of the well and the transducer cable was taped to the outer casing of the well. 3) The slug was submerged below the water table in the well, above the pressure transducer. 4) The water level was given sufficient time to recover back to hydrostatic conditions. 5) A logarithmic water depth sampling schedule was started using the transducer and then the slug was quickly removed from the well. 6) The test was terminated when water level returned to hydrostatic conditions.

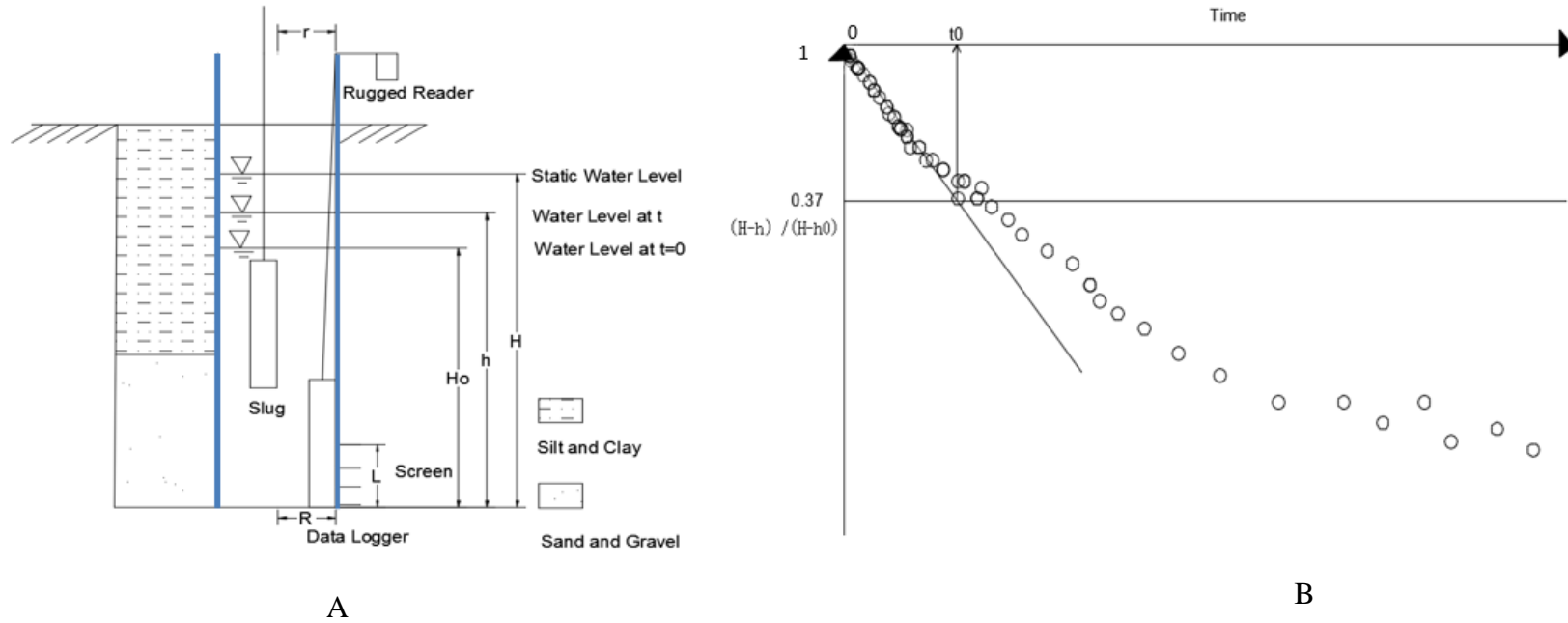


Figure 13: A. The illustration of the slug test. B. Schematic illustration of Hvorslev analysis

All of the wells were installed in the fine sand layer according to the layer stratification in the model (Figure 5). The slug test gives an estimated measurement of hydraulic conductivity, and can be used to constrain the calibration exercise.

Hvorslev (1951) developed a mass-balance expression for flow into or out of a well.

$$\pi r^2 \frac{dh}{dt} = FK(H - h) \quad (3.4)$$

where r is inner borehole radius; h is the head in well; t is the time; H is the static water level outside of the well; K is the hydraulic conductivity; F is the shape factor. Based upon the mass balance equation, Hvorslev developed the follow analytical solution to 3.4 using the method of ‘separation of variables’ for the isotropic aquifer condition. (Shape factor F is determined numerically.)

$$K = \frac{r^2 \ln(L/R)}{2Lt_0} \quad (3.5)$$

where K is the hydraulic conductivity; r is the radius of the inner tube; R is the radius of the well and gravel pack; L is the length of the perforated screen; t_0 is the time when the plotted asymptotic line (time vs $(H-h)/(H-H_0)$) reaches the straight line $((H-h)/(H-H_0)=0.37)$ (Figure 13B).

There are some limitations to this method. The hydraulic conductivity determined using this approach is only applicable to sediments within about 1m from the well. Additionally, it assumes that the slug is instantaneously removed from the well and then recovery occurs. If the formation is very permeable, the recovery can begin while the slug is being removed, oscillations in water levels in the well can also occur in very permeable sediments (Springer and Gelhar, 1991). Moreover, this analytical solution is based on the drawdown/recovery for non- radial flow in a homogeneous aquifer, water table outside of the well is assumed to be static.

3.2.3 The Specific Storage Estimation

Specific storage is the amount of water released from storage, produced from a unit volume of aquifer, for a unit change in hydraulic head (Freeze and Cherry, 1979). Specific storage at this site is estimated by hydrograph analysis, based on the barometric effect (BE) (Spane, 2002). The higher the barometric pressure, the lower the groundwater table and vice versa. Assuming Terzaghi’s law is valid, in a confined aquifer, the barometric pressure along with the weight of the low permeability layer is supported by the groundwater fluid pressure and the effective stress on the matrix. When the barometric pressure increases, part of the pressure is supported by the matrix. In the well, however, the pressure increase is solely supported by the water column. The pressure difference on the water between the well and aquifer pushes the water column in the well into the aquifer, lowering the water level in the well. Specific storage can be extracted by measuring the barometric pressure in the atmosphere and the groundwater table change in the well. We will use wells w3 to w5 for the calculation. These wells are in the area that

has silty clay on top which makes the aquifer at this region show confined aquifer features. These wells are far from the river, and show less impact from river stage changes. The groundwater table has a very clear inverse relationship with the barometric pressure during the period Feb, 2013 to Apr, 2013 (Figure 17).

The specific storage can be estimated by the equation below:

$$BE = \frac{\gamma_{water} \Delta h_{well}}{\Delta p_{atm}} \quad (3.6)$$

$$S_s = \frac{\gamma_{water} n \beta}{BE} \quad (3.7)$$

where BE is the barometric effect coefficient; γ_{water} is the specific gravity of water (1N/L); Δh_{well} is the groundwater table change in the respective well; Δp_{atm} is the atmospheric pressure change of the site at well4; n is the porosity of the aquifer (assumed 0.3 here); β is the compressibility of water ($4.6E-10 \text{ m}^2/\text{N}$); S_s is the specific storage of the aquifer. The BE is calculated in each well selected, and the specific storage is also calculated for each well. Finally, we used the average S_s of the three wells to represent the research site.

3.2.4 Evapotranspiration

Evapotranspiration is estimated in two ways in this research: the Kimberly Penman method, and using remote sensing by checking Normalized Difference Vegetation Index (NDVI) values. The maximum evapotranspiration (ET) data used in the ETS package in MODFLOW model for the whole area is from the RAWS climate station in Bosque del Apache calculated using the Kimberly Penman's equation (3.8) (Docter, 1994). The averaged ET over the study period was applied in the ETS package as the maximum ET every day.

$$\lambda ET_r = \frac{\Delta}{\Delta + \gamma} (R_n - G) + \frac{\gamma}{\Delta + \gamma} 6.43 W_f (e_s - e_a) \quad (3.8)$$

where Δ is the slope of the saturation vapor pressure-temperature curve; γ is the psychrometric constant; R_n stands for the net radiation; G is the soil heat flux; W_f represents the dimensionless wind function; e_s is the average saturation vapor pressure; e_a is the saturation vapor pressure; λ is the latent heat of vaporization of water; ET_r is the reference ET for short crops. The Kimberly Penman method is a combination equation which combines the net radiation and advective energy transfer into one equation (Dockter, 2008) using the weighting factors for these two influential factors. It assessed the relative importance of these two impacts.

Change in biomass is another measure of evapotranspiration. The density variation of vegetation and the vegetation type can be used to estimate evapotranspiration. NDVI is an indicator that distinguishes these differences and estimates the ET rate spatially (Figure 19). Red and near infra-red were the two spectrums in NDVI calculation, Landsat 7 and Landsat 8 images were used in the existing NDVI calculation module in ERDAS (2013). For Landsat 7, band 3 (red) and 4

(near infrared) were used in the calculation, while for Landsat 8 images, band 4 (red) and 5 (near infrared) were used. Extra ET applied in some specific high evapotranspiration regions of the research site is based on the NDVI by adding extra discharge in the first layer.

The calculation from NDVI to ET (Palacios-Velez & Flores-Magdaleno, 2013; Labbassi et al, 2013):

$$K_c = 1.25 \times NDVI + 0.2 \quad (3.9)$$

$$ET = K_c \times ET_o \quad (3.10)$$

where K_c is the crop coefficient calculated from NDVI; ET_o is reference ET (Kimberly Penmen ET_o), while ASCE ET_o is recommended (Pessarakli, 2014), ET_o difference by these two methods is 0.003 m/d which will not make a big difference on the groundwater modeling results; ET is the estimated actual ET.

3.2.5 The Pumping/Irrigation Rate Estimation

Riparian land along Rio Grande has a long history of irrigation. In the MODFLOW 3D model, these are assumed to be chile fields on the west side of the research domain, west of the Rio Grande. There are 8 pumping wells in the research area according to the Office of the State Engineer. Six wells are located in the irrigation field side (Figure 1B). The other two wells are on the wetland side. According to site investigation, two wells in the wetland side are abandoned in recent years, so no pumping was considered from them for the modeling period. We assumed that the amount of pumping equal to the water demand by the crops on the agricultural fields. We did not account for runoff from drainage system. The pumping period is assumed to be uniform from June to November of each year, 153 days, which is a reasonable time period for chili growth in middle Rio Grande (Bosland & Walker, 2014). We removed a portion of the applied water using calculated ET.

The equation used for the consumptive use estimation is by the Blaney-Criddle (Blaney & Criddle, 1949) method. It is a method to estimate the water consumption by plants considering the temperature, length of the day and the moisture availability influences. Equation is stated as below:

$$u = kp \frac{45.7t+813}{100} \quad (3.11)$$

where k is the empirical consumptive-use crop coefficient for the irrigation season or growing period; p is monthly percentage of daytime hours of the year (Table 15); t is the mean monthly temperature in Celsius; u is the monthly consumptive use in millimeter. The calculated average irrigation rate is a very conservative value, because the crops in this site may not all be chile. The water calculated here is only the water that is needed for the plants to develop regardless of the water drained back to river and the water goes down to the underground aquifer. This approach does not consider many other factors, such as the net radiation, the wind speed, etc. In order to test the influence of the pumping activity on the groundwater tables of east wetland side, a sensitivity analysis is given in the discussion section.

3.3 Groundwater Model

3.3.1 1D Transient Numerical Model Based on Rorabough Equation

According to the field data, the groundwater table levels in the research site are strongly affected by the Rio Grande stage change (Figure 10). We developed a one-dimensional transient groundwater flow model to determine to what extent water-level fluctuations in the wetland are controlled by river stage. This analysis is analogous to the approach taken by Rorabaugh (1964). We solved the following one-dimensional transmissivity-based groundwater flow equation:

$$S_s \frac{dh}{dt} = T \frac{d^2 h}{dx^2} + R(t) \quad (3.12)$$

where S_s is the specific storage; h is the head (water table); x is the distance; T is the transmissivity (hydraulic conductivity times thickness); $R(t)$ is the sum of precipitation (positive) and evapotranspiration (negative) on each day during the modeling period. The one-dimensional transient model is an equation which is based on the assumption that the river and the confined aquifer are in good hydrologic convection.

Equation (3.12) is solved using the finite difference method assuming an implicit time scheme:

$$S_s \frac{h_i^{k+1} - h_i^k}{\Delta t} = T \frac{h_{i+1}^{k+1} - 2h_i^{k+1} + h_{i-1}^{k+1}}{\Delta x^2} + R(t) \quad (3.13)$$

$$-\frac{T\Delta t}{S_s \Delta x^2} h_{i-1}^{k+1} + (1 + 2 \frac{T\Delta t}{S_s \Delta x^2}) h_i^{k+1} - \frac{T\Delta t}{S_s \Delta x^2} h_{i+1}^{k+1} = h_i^k + \frac{R(t)\Delta t}{S_s} \quad (3.14)$$

where i denotes node number; k denotes the time level; S_s is the specific storage; h is the head (water table); Δt is the time step; Δx is the distance between two nodes; T is transmissivity; $R(t)$ is the sink term (Precipitation+Evapotranspiration) (Figure 14).

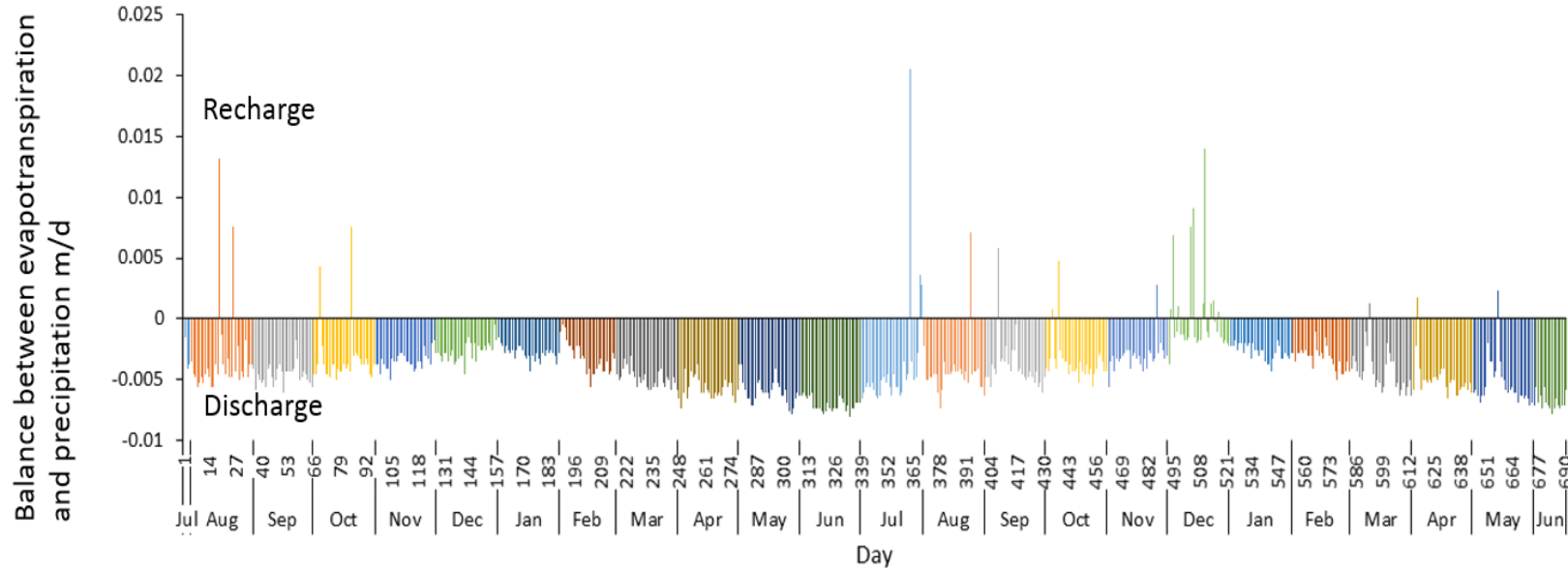


Figure 14: $R(t)$ values used in the one dimensional numerical model. It is the balance between the evapotranspiration and precipitation, recharge occurs when precipitation is larger than evapotranspiration calculated using the Kimberly-Penman equation, discharge occurs when evapotranspiration is larger than the precipitation.

We solved this equation using a finite difference method in MATLAB. The time step is 1 day in over a total 689 day period. The transect spans from the Rio Grande channel to the east boundary, and has a distance of 1350 meters. The distance between each node is 5 meters (Δx). The river stage is specified on the west edge of the transect (node1). River stage changes at every time step. The east side of the model is assumed to be no-flux boundary. The heads in the model were assumed to vary. The initial groundwater table is set to linearly change from the Rio Grande to the east side boundary as the initial condition (1395.3m, Anderholm, 1987). A sensitivity analysis was performed by changing one influential factor, while keeping others fixed.

Spatial variation in S_s , $R(t)$ and T were neglected. The one-dimensional numerical model was used to assess the extent of influence from river on the groundwater tables. Other factors that influence water table fluctuation such as stratigraphic hydrogeologic layers, pumping/irrigation, regional high evapotranspiration, etc. were not considered in this analysis.

3.3.2 Numerical Model in MODFLOW

A more general three-dimensional numerical model was constructed using MODFLOW and applied to assess the influences of multiple hydrostratigraphic layers, spatial and temporal variations in ET, down-valley groundwater flow, among other factors. The calibrated model results were used to delineate the wetland.

The governing groundwater flow equation for the three-dimensional numerical model is shown as below (McDonald & Harbaugh, 1988):

$$\frac{\partial}{\partial x} \left(K_{xx} \frac{\partial h}{\partial x} \right) + \frac{\partial}{\partial y} \left(K_{yy} \frac{\partial h}{\partial y} \right) + \frac{\partial}{\partial z} \left(K_{zz} \frac{\partial h}{\partial z} \right) = S_s \frac{\partial h}{\partial t} + R(t) \quad (3.15)$$

where h is the groundwater-table elevations; K_x , K_y , K_z in the equation are the hydraulic conductivities on x , y and z directions respectively; S_s is the specific storage of the aquifer; $R(t)$ is the source/sink term at each node; t is the time (McDonald & Harbaugh, 1988). The ETS package, drain package, river package equations were incorporated into this governing equation later in order to assess the influences of these factors.

3.3.2.1 Model Domain/Discretization

The MODFLOW model covers the research area which includes both the east wetland site and west irrigation side with the Rio Grande in the middle. Irrigation and pumping are represented in the west irrigation site only. The block-centered finite-difference cell sizes varied in the x and y directions. The grid was composed of 150×150 nodes in the x and y direction. The domain length in the east-west direction is 3507 m on average. The domain length in the north-south direction is 4426 m on average. Length of each FDM cell in the x direction (Δx) is 23.4 m. The length of each FDM cell in the y direction (Δy) is 30 m. There are four vertical layers in this model. The top unit is considered to be a low permeability layer composed of 3 meters of organic matter, the second layer consists of 6 meters of higher permeability sands. Third layer is a 1 meter

thin low permeability layer detected by SSPA (2004a). The fourth layer is 14 meters thick and assumed to be composed of gravel and sand (high permeability layer). The production wells are completed in this lowest unit.

3.3.2.2 Boundary Condition

Boundary conditions are very important in any groundwater flow model. They determine, in part, the groundwater levels within the site.

On east wetland side of the model, the groundwater table decreases from the Rio Grande to the east boundary. This suggests limited inflow from the east boundary (Figure 10) and evapotranspiration. On the west side of the model domain, we also assumed a no-flow boundary. The north boundary is set to be a specified-flux boundary by installing pseudo wells. These injection wells are located in every cell on the north boundary. Each well has the same injection rate (Figure 15). The value of the inflow was estimated using the region hydraulic gradient and a calculated transmissivity (3.16; 3.17). The injection wells are included in all four layers. The flux was varied at the boundary equal to match the Anderholm's water table elevation data. At the south side of domain, the boundary is set to be a specific-head boundary in accordance with Anderholm's water-table map. (Figure 9; Figure 15)

Water heads information for the four corners is from the linear interpolation from (Anderholm 1987) observed heads contour (Figure 9).

Locations	Northwest	Northeast	Southwest	Southeast
Heads m	1396.6	1402.1	1389.9	1389.3

Table 4: Observed heads on four corners.

For the calculation of the injection rate at the north boundary, we used the Darcy flux (3.19) based on our estimation of effective hydraulic conductivity (3.16) for the 4 layers and the north-south regional head gradient. The calculation is based on equation below:

$$K_e = \frac{\sum (L_i \times K_i)}{\sum L_i} \quad (3.16)$$

$$H_{up} = \frac{NW + NE}{2} \quad (3.17)$$

$$H_{down} = \frac{SW + SE}{2} \quad (3.18)$$

$$Q = \frac{Aq}{n_w} = -K_e \frac{\Delta h}{D_{BB}/n_w} = \frac{(H_{up} - H_{down})/D_{BB} \times K_e \times SAA'}{n_w} \quad (3.19)$$

where K_e is effective hydraulic conductivity; L_i is the thickness of layer i ; K_i is hydraulic conductivity of layer i ; Aq is the total volume of water injected by the pseudo wells; n_w is the number of wells on the upper boundary line. Δh is the heads difference at two locations; H_{up} is the averaged observed head at the north boundary (3.17); H_{down} is the averaged observed head at the south

boundary (3.18); $D_{BB'}$ is the distance from B to B' (Figure 15), $S_{AA'}$ is the area of the cross section along A to A' (Figure 15),

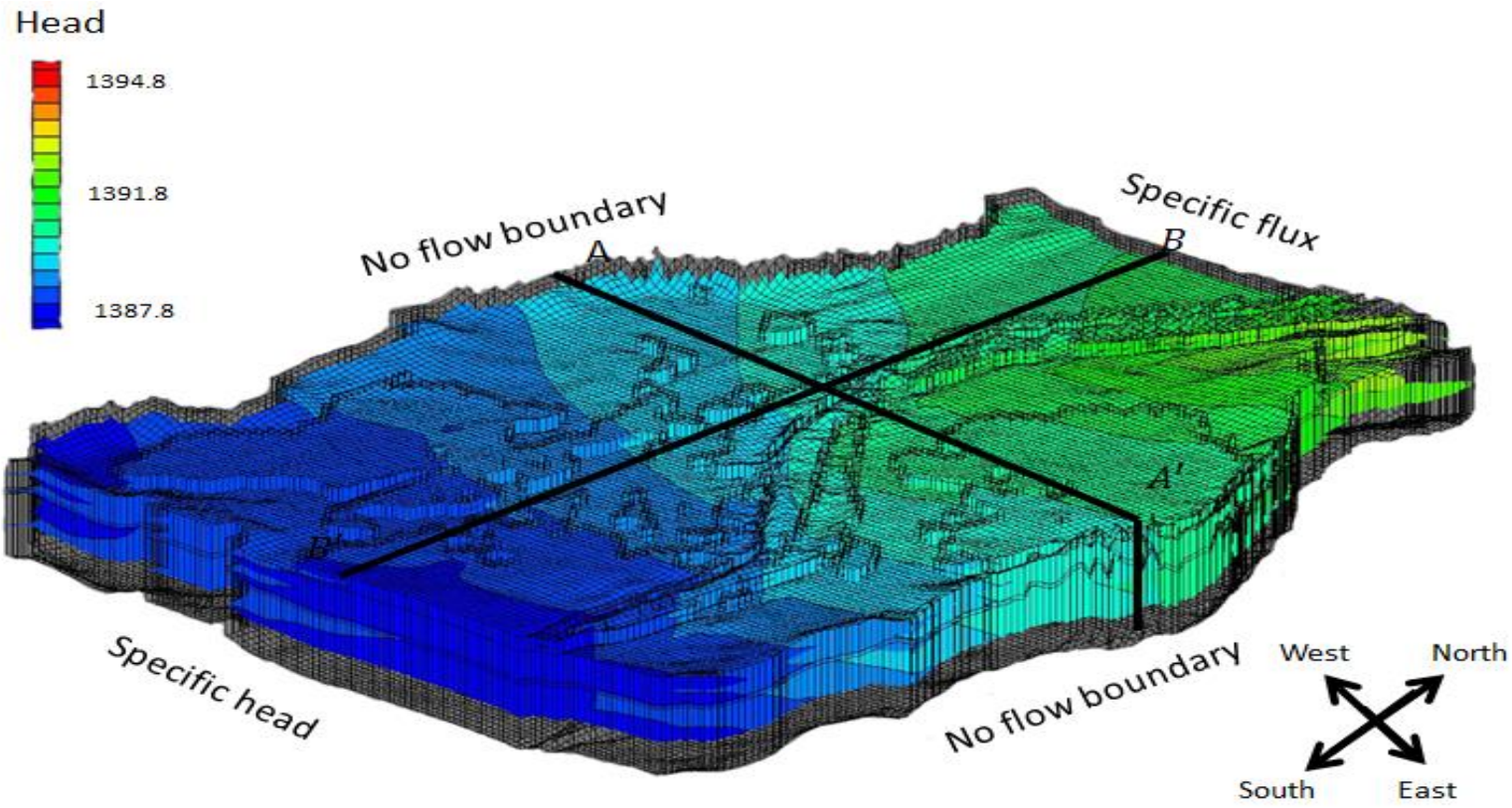


Figure 15: Boundaries and layers of the research site (The depth has been exaggerated by 20, different colors represents different water table elevations)

3.3.2.3 The Rio Grande River Stage

Rio Grande discharge comes mostly from the mountain snowmelt in the upper Rio Grande catchment in southern Colorado and northern New Mexico. In addition to snowmelt, the river stage is also affected by pumping, irrigation, ET and precipitation.

The river package in MODFLOW was used to represent the effects of groundwater surface water interaction within the study area. Equation used in the river package is given by (McDonald & Harbaugh, 1988):

$$QRIV = CRIV(HRIV - HAQ) \quad (3.20)$$

where QRIV is the river water leakage through the riverbed; CRIV is the riverbed water conductance; HRIV is the head elevations of the river; HAQ is the groundwater-table elevations in the aquifer right below the riverbed (McDonald & Harbaugh, 1988).

The conductance of the riverbed (CRIV) along the Rio Grande has been estimated by Cardenas (2006). The head in the aquifer beneath the riverbed (HAQ) is calculated in the model at every time step, and the head on the river side of the riverbed (HRIV) is interpolated at every node along the river from the two ends (north/south) of the river at this research site. The river stage is recorded at two river gauge stations along the Rio Grande (Figure 1A). In our model, the river domain stage was specified at the north and south ends of our model based on the interpolated river stage data from the two gauging stations at Escondida and San Antonio, NM. The gauge to the north nearest to this site has a station ID of 08355050, near Escondida. The gauge to the south is 08355490 in San Antonio. The location of USGS 08355050 river gauge station is 34°07'15"N, 106°53'13"E (NAD83). Stage data is available from October, 1st 2007 to current. The San Antonio station which is located down river at 33°55'36"N, and 106°51'04.2"E. Available data starts from October 1st 2007 at the station. The distance from the north end of the model to the Escondida gauge is 11859 m. The distance from the southern border of the model to the San Antonio gauge station is 6026 m. Based on the distance and the recorded river stage at the two gauging sites, the river stage at the north and south ends of the model domain were linearly interpolated.

$$Hr1 = H1 - \frac{H1-H2}{Dt} \times D1 \quad (3.21)$$

$$Hr2 = H2 + \frac{H1-H2}{Dt} \times D2 \quad (3.22)$$

where Hr1 is the stage of the river at the north end of the section; Hr2 is the stage of the river at the south end of the section; H1 is the river stage recorded at the station USGS 08355050 (Escondida); H2 is the river stage at the station USGS 08355490 (San Antonio); Dt is the distance from the station USGS 08355050 to USGS 08355490; D1 is the distance from the station USGS 08355050 to the North end; D2 is the distance from the station USGS 08355490 to the south end. Values of D1, D2 are listed in Table 5.

In this interpolation, it is assumed that surface water elevation varies linearly downstream. The precision of the river-stage data imposed at the two ends of the model domain are questionable. We varied river stage as part of a sensitivity study.

	Distance m	Weight
Distance from Escondida station to A m, and weight (D1)	11859	0.54
Distance from San Antonio station to B m, and weight (D2)	6026	0.28
Total distance from 08355050 to 08355490 m, and weight (D1+D2)	21882	1

Table 5: Distance between stations and locations in the site

3.3.2.4 The Description and Properties of the Low Flow Conveyance Channel

The Low Flow Conveyance Channel (LFCC) (Figure 1B) is an irrigation drain intended to conduct water to Elephant Butte reservoir near T or C, NM which runs parallel along the river. It plays an important role in controlling the near-surface groundwater flow direction and water-table elevation. It is a drain on the irrigation side of the research area (west side) (Shafike, 2004).

We used the drain package in MODFLOW to simulate the effects of the LFCC. The equation for the drain package is shown as below (McDonald & Harbaugh, 1988):

$$QD_{i,j,k} = CD_{i,j,k}(h_{i,j,k} - d_{i,j,k}) \quad (3.23)$$

where $QD_{i,j,k}$ is the water flow rate from field to the drain; $CD_{i,j,k}$ is the water conductance between the aquifer and the drain; $h_{i,j,k}$ is the groundwater-table elevations in the aquifer near the drain; $d_{i,j,k}$ is the water-table elevations in the drain (McDonald & Harbaugh, 1988). Conductance between the aquifer and the drain ($CD_{i,j,k}$) is from the reference paper and adjusted in the model (Richard, 2006), as of 3.048 m/d. The head in the aquifer near the drain ($h_{i,j,k}$) is calculated in the model at every time step. The head in the drain ($d_{i,j,k}$) is assumed as the drain bed elevation as initial condition. Elevation of its bed is designed to be 5.2 m lower (Richards, 2006) than the Rio Grande river bed at every location. The elevation of the drain bed linearly decreases from north to south.

3.3.2.5 MODFLOW Evapotranspiration Module

The ETS module was used in MODFLOW to represent groundwater supported evapotranspiration. When $SURF \geq h \geq SURF - EXDP$, the equation used for evapotranspiration calculation in the module is stated as below (McDonald & Harbaugh, 1988):

$$Q = EVTR(h - (SURF - EXDP))/EXDP \quad (3.24)$$

where Q is the ET rate; EVTR is the maximum ET rate at the land surface; h is the groundwater-table elevations in the aquifer; SURF is the land surface elevation; EXDP is the extinction depth of evapotranspiration (McDonald & Harbaugh, 1988).

Evapotranspiration consumes a large sum of water every day in semiarid regions. In this model, ET data is from RAWS station in Bosque del Apache, calculated by Kimberly Penman equation. The averaged ET over the study period is applied in this

model as the maximum ET incorporated in ETS package. Extinction depth is set to be 3 meters. The maximum ET occurs when the simulated water table reaches SURF, ET decreases linearly until reaches the extinction depth (EXDP). In addition, in some regions, maximum ET is higher than the averaged ET due to the vegetation density variation, vegetation types, groundwater depth, etc. The Normalized Difference Vegetation Index indicates the ET difference in different regions. By looking at the NDVI map converted from the Landsat images at this site, after the calculation of ET from NDVI, the highest ET regions usually have a 0.001m/d higher ET rate than other regions. The higher ET rate is applied in the highest ET regions recognized by the NDVI map by adding a discharge rate of 0.001m/d in the first layer.

3.3.2.6 Pumping and Irrigation

Pumping and irrigation activities are on the west side of the river. Because no pumping-rate data were recorded, we estimated pumping based on water demand using the Blaney-Criddle equation.

At this site, various crops are cultivated on the west irrigation field, such as chile, alfalfa, and hay. In order to estimate maximum pumping, chile was assumed as the only crop covering the fields. The six pumping wells are used for irrigation on west side. Pumping water ($1120 \text{ m}^3/\text{d}$) was assumed to be withdrawn from layer 4, and immediately applied on layer1 by adding as part of recharge rate. The pumping rate calculated by this method is a very conservative number, as flood irrigation is the mainstream irrigation technique in this area. Additionally, groundwater/surface-water interaction, water drainage, weather condition and so on could also interfere with the needed water amount. In order to find out the pumping influences and the assumption applicability, a sensitivity analysis of pumping is performed and discussed later in this model.

3.3.2.7 Recharge on the Site

Recharge sources are different for the two sides of the study area. It is one of the important factors controlling groundwater table elevations. On the west irrigation land, recharge is the sum of precipitation and applied irrigation water minus the average maximum ET daily (3.25). On the east side of the model domain, recharge is calculated by taking the precipitation minus the average maximum ET (3.26). Negative recharge is set to be 0 on both sides. These are the transient recharge values on daily basis.

$$Rw = P + I - PETmax \quad (3.25)$$

$$Re = P - PETmax \quad (3.26)$$

where P is the precipitation recorded in RAWS weather station situated in Bosque del Apache; I is the irrigation rate calculated from crop needs based using Blaney-Criddle method; PETmax is the maximum potential ET calculated using Kimberly Penman method; Rw is the recharge rate on the west side; Re is the recharge rate on the east side.

3.3.2.8 Layer Properties

Hydrostratigraphy and associate hydraulic properties are important factors controlling the groundwater table fluctuation, groundwater recharge rate and groundwater consumption, etc. The layers properties are determined both by the borehole logs across the research site from east to west, named Brown Arroyo Transect, that was made available by SSP&A (Figure 5), and the slug test described in the last section. According to the geological description in chapter2, there are four layers in this site. The basic layers hydraulic conductivities and porosities are adjusted from former researches and tested in this model. Some other layer properties, such as specific yield and specific storage, are from the discussion above. Properties of different layers used in this model are shown as below (Table 6).

Earth layer properties						
Layer number	Horizontal K (m/d)	Vertical anisotropy	Thickness m	Porosity	S_y	$S_s(1/m)$
Layer1	7	4	3	0.3	0.1	5E-6
Layer2	220	2	6	0.3	0.2	5E-6
Layer3	20	3	1	0.3	0.1	5E-6
Layer4	150	2	14	0.3	0.2	5E-6

Table 6: Layer properties in research site

CHAPTER 4

RESULTS

4.1 Specific Storage Estimation

Specific storage was estimated by relating changes in barometric pressure to water level fluctuations (Spane, 2002) using equations (3.7). The period of record used here was from 03/02/2013 to 04/27/2013 for wells w3, w4, w5. These wells are far from the Rio Grande with a confining unit on top. The influence from the river is damped in these wells. River stage doesn't show a strong correlation with the groundwater table elevations in wells during this specific period (Figure 16, Figure 17). We converted barometric pressure to pressure head in meter. The open circles in Figure 17 are the data chosen for calculation. The inverse relationship between barometric pressure and the groundwater table level is apparent in Figure 17.



Figure 16: The river stage during the specific period used for the specific storage analysis.

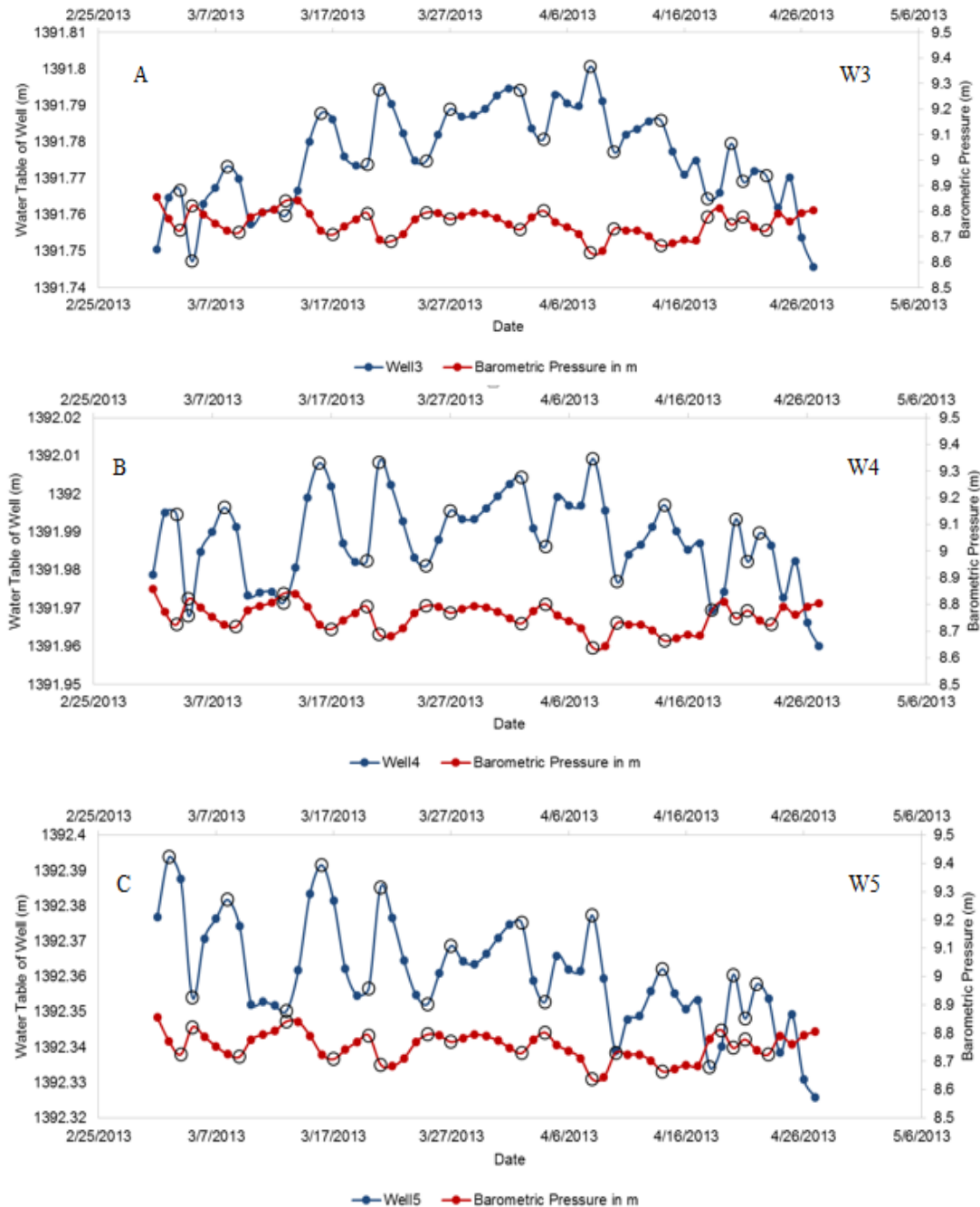


Figure 17: Inverse correlation between barometric pressure change and water table fluctuations in wells, w3, w4 and w5.

Table 7: Range of S_s in each well

	Min. S_s	Max. S_s	Mean S_s
w3	2.6×10^{-5}	1.1×10^{-4}	6.8×10^{-5}
w4	1.8×10^{-6}	9.6×10^{-6}	5.0×10^{-6}
w5	2.2×10^{-6}	9.1×10^{-6}	4.6×10^{-6}

Variables	γ_{water} KN/m ³	n	β m ² /N	S_s 1/m
Values	10	0.3	4.6×10^{-10}	5.0×10^{-6}

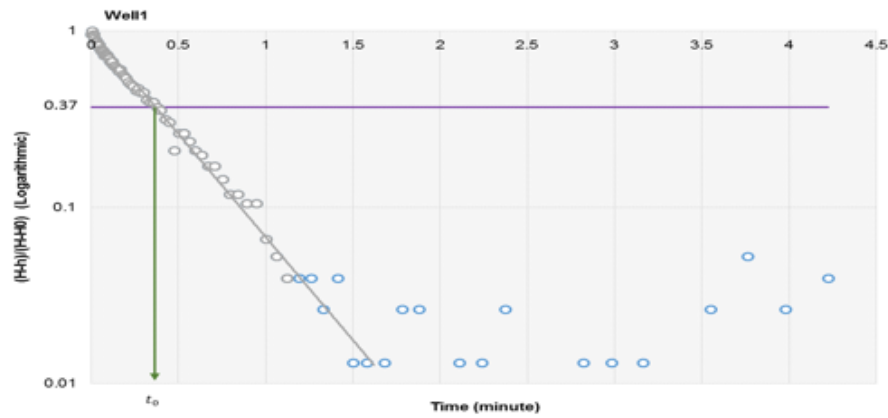
Table 8: Parameters used in the specific storage calculation

The changes in barometric pressure and water levels in wells are compared and calculated to derive the barometric effect coefficient. Based on the relationship between barometric coefficient and specific storage equation (3.6), the specific storage is calculated in each of the selected wells, w3, w4, w5 (Table 7), varies between 1.8E-6 1/m and 1.1E-4 1/m. 5E-6 1/m (Table 8) is used in the model for every layer. By calculating the groundwater-table fluctuations based on the specific storage and comparing with the observed ones, it shows a close match. Additionally, it is a similar value to the specific storage used in Richard (2006) (10^{-5} 1/m).

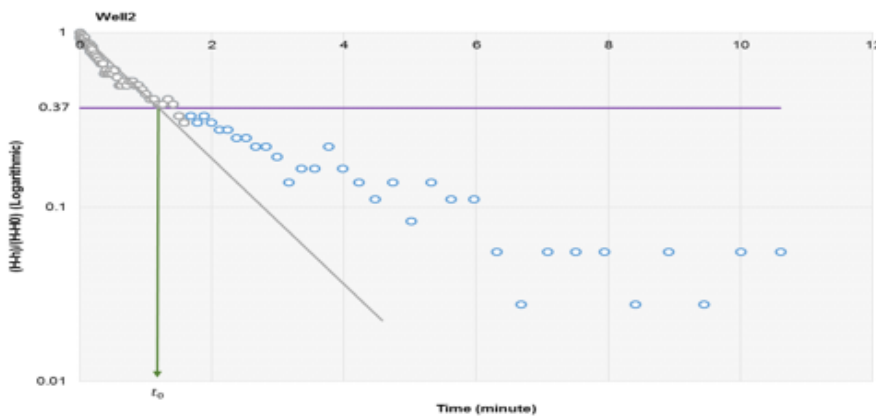
The specific storage calculated is likely only representative of conditions around these selected wells.

4.2 Slug Tests

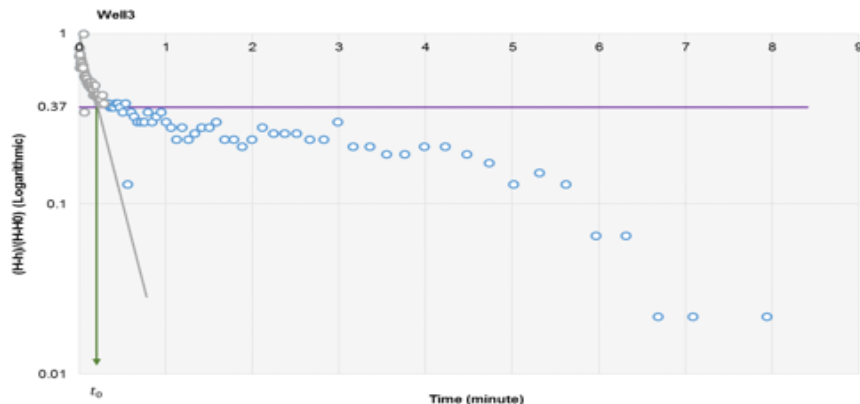
Slug tests were conducted to estimate the hydraulic conductivity of the uppermost fine sand layer within wells w1 to w3. The In Situ Level TROLL 700 pressure transducer has a precision of 0.01 ft. Depths data were recorded for up to 10 minutes. Hydraulic conductivity was calculated using the Hvorslev method equation (3.5), finding the time (t_0) associated with a dimensionless draw down of 0.37 (Figure 13B, Figure 18). This aquifer test assumes that the aquifer is homogeneous, and hydrostatic conditions occur outside of the well (Hvorslev, 1951). The hydraulic conductivity from an individual well can only represent the conductivity of its surrounding area within about 1 meter.



A. Slug test in well1



B. Slug test in well2



C. Slug test in well3

Figure 18: Homogenized slug test measurements in three wells

The calculated hydraulic conductivity varied between 5 and 32 m/d in wells w1 to w3.

Well ID	t_0 (s)	Hydraulic conductivity K (m/d)	The slug volume calculated based on maximum drawdown during slug test (m^3)	Slug volume (m^3)
W1	21	16	4.66×10^{-5}	8.34×10^{-5}
W2	71	5	2.21×10^{-5}	8.34×10^{-5}
W3	11	32	2.82×10^{-5}	8.34×10^{-5}

Table 9: Hydraulic conductivity calculated in each well

These values seem reasonable. The hydraulic conductivity for unconsolidated well-sorted sand and gravel ranges from 3 m/d to 304 m/d (Bear, 1972). The calculated values rest in this range. Freeze & Cheery (1979) gave a range of 0.3 m/d to 274 m/d for clean sand. Later 300 m/d and 220 m/d are used in the one-dimensional and three-dimensional models respectively, for the scale effect (Schulze-Makuch et al., 1999). And the test model demonstrated that the 300 m/d and 220 m/d were the best values for the uppermost sandy layer. The volumetrically calculated slug volume is bigger than the displaced volume calculated from the maximum drawdown in water table in wells. This suggests that the aquifer began to recover very soon. This is a potential source of error.

4.3 Evapotranspiration

Evapotranspiration rates were calculated in two ways: the Kimberly Penman energy balance method and Normalized Difference Vegetation Index (NDVI) analysis based on Landsat images. The potential evapotranspiration calculated using Kimberly Penman method is assumed to be representative of the entire field site. This value was assigned to the ETS package in MODFLOW as the maximum ET rate at land surface (0.004 m/d).

Because of the vegetation type and density varies across the study area, Landsat images analysis provides estimation of spatial variation in evapotranspiration (Figure 19). By checking the NDVI map from Landsat image analysis, there are some higher evapotranspiration regions on the wetland side. Different pseudo colors were assigned to different NDVI ranges (Figure 19, Table 10). The NDVI was estimated for the highest ET regions and lowest ET regions, and the evapotranspiration difference between the highest ET region and the lowest ET region is listed in Table 11. For most days of a year, the highest ET regions have 0.001m/d higher ET than the lowest ET regions.

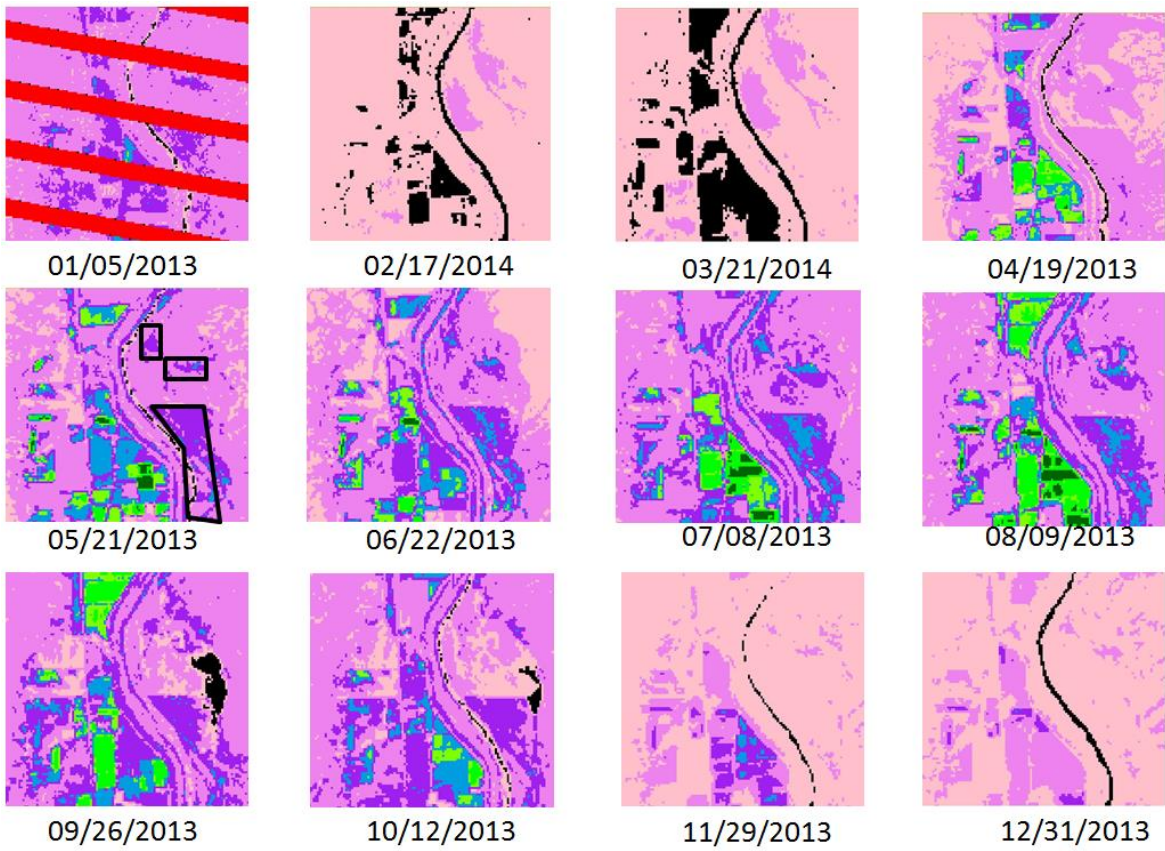


Figure 19: Normalized Difference Vegetation Index images in each month (The selected areas as high ET zones are enclosed in the polygons in image. 05/21/2013. They are consistent in images of other months.)

Color	Black	Pink	Violet	Purple	Map Grid Blue	Chartreuse	Green	Dark Green
NDVI	<0	0-0.1	0.1-0.2	0.2-0.3	0.3-0.4	0.4-0.5	0.5-0.6	0.6-0.7

Table 10: Colors in NDVI maps and their corresponding NDVI ranges

Month	ET_r m/d	Base color NDVI	ET m/d	High ET zone Color NDVI	ET m/d	ET difference m/d
Jan	0.00093	0.15 6	0.0003	0.25	0.00048	0.00012
Feb	0.0047	0.05	0.0012	0.15	0.0018	0.00058
Mar	0.0057	0.05	0.0015	0.15	0.0022	0.00071
Apr	0.0049	0.15	0.0019	0.25	0.0025	0.00061
May	0.0061	0.2	0.0027	0.35	0.0039	0.0011
Jun	0.0072	0.2	0.0032	0.35	0.0046	0.0013
Jul	0.0058	0.2	0.0026	0.35	0.0037	0.0011
Aug	0.0053	0.2	0.0024	0.35	0.0034	0.001
Sep	0.0047	0.15	0.0018	0.35	0.003	0.0012
Oct	0.0043	0.1	0.0014	0.25	0.0023	0.00082
Nov	0.002 4	0.05 2	0.0005	0.1	0.00067	0.00013
Dec	0.0028	0.05	0.0007	0.1	0.0009	0.00017

Table 11: ET calculated in each month based on NDVI

4.4 The Pumping/Irrigation Rate Estimation Using Blaney-Criddle Method

We used the Blaney-Criddle method for ET consumption to estimate pumping requirements for the irrigated fields to the west of the Rio Grande.

We assumed chiles were grown in this field. According to Brouwer & Heibloem, 1986, chile peppers have four growing stages. They are the initial stage, crop development stage, mid-season stage and late season stage. Generally, the number of days for chile to grow through these stages varies between 120 and 210 days (Table 12). Research site is located in the middle Rio Grande. In this region, the duration of chile growth from germination to harvest is 153 days on average from June 1st to Oct 30th (Table 14; Bosland & Walker, 2014).

Plant type	Growing stages	Total	Initial stage	Crop Development stage	Mid-season stage	Late season stage
Chile pepper	Minimum growing days	120	25	35	40	20
	Maximum growing days	210	30	40	110	30

Table 12: Days of different growing stages of chile. (From Brouwer & Heibloem, 1986).

Plant type	Growing stages	Initial stage	Crop dev. stage	Mid-season stage	Late season stage
Chile pepper	Crop coefficient	0.35	0.70	1.05	0.90

Table 13: The crop coefficient for chili at different stages (From Brouwer & Heibloem, 1986).

The number of days for every growing stage for chile in middle Rio Grande is interpolated by the percentage of days in each stage over the whole period considering both minimum and maximum days (Table 12; Table 14).

Total	Initial stage	Crop dev. stage	Mid-season stage	Late season stage
153	26	37	64	26

Table 14: Interpolated days of each stage for chile in middle Rio Grande

In order to calculate the crop coefficient for each month required by the Blaney-Criddle equation, the crop coefficient for each month is interpolated by equation as below.

$$Kc = \sum \frac{Di}{Mi} Kc_i \quad (4.1)$$

where Di is days in a specific (ith) month that is in growing stage i, Mi is the total number of days of the ith month, Kc_i is the crop coefficient of stage i (Table 15), Kc is the crop coefficient of the specific month. The area of the irrigation site is roughly calculated in Google Earth as $4.9 \times 10^7 m^2$.

With the data obtained from above, the evapotranspiration rates are used to estimate the pumping rate required to support the crops within the irrigated fields on the west side of the model domain.

Month	Kc	P	T(C)	Pumping rate (m^3/d)	Pumping rate average (m^3/d)
Jun	0.17	9.7	25	890	1200
Jul	0.22	9.88	27	1200	
Aug	0.39	9.33	23	1800	Evapotranspiration rate average (m/d)
Sep	0.40	8.36	20	1600	0.0015
Oct	0.19	7.9	14	570	

Table 15: Calculated averaged evapotranspiration using Blaney-Criddle equation and its corresponding averaged pumping rate during growing season (p is from Blaney-Criddle, 1942, Table 1)

4.5 1D Numerical Model Using Rorabaugh Equation

Groundwater table levels are highly correlated to Rio Grande stage height (Figure 10). In order to assess the extent of influence from Rio Grande, a one-dimensional numerical model loosely based on the Rorabaugh (1964) analytical solution was constructed in MATLAB. The analysis differs from Rorabaugh (1964) in that a source/sink term was included to account for evapotranspiration demand on the aquifer.

Lateral average water levels in the monitoring wells furthest from the Rio Grande were lower, on average, than the river stage. The model transect runs across the wells in the research area from the river to the east wetland side with 5 m distance interval between each node. In this model, a time-varying specified head boundary condition was imposed at the location of the Rio Grande. A no-flux boundary condition was imposed on eastern edge of the model domain. The initial groundwater table for each node along the transect is interpolated from the east boundary node at 07/28/2010 to the river node linearly. Additionally, balance between discharge (evapotranspiration) and recharge (precipitation) $R(t)$ (Figure 14) is also incorporated in the model. It is a sink term at all nodes that changes at every time step. In this model, the most important factors controlling the groundwater-table elevations are river stage, hydraulic diffusivity, and the recharge term $R(t)$. The mean value of $R(t)$ over the study period was -0.004m/d. This model further confirmed the dominant influence of the river stage. By matching the phase lag and amplitude of the groundwater fluctuations in wells, this model provided a rough estimation of the hydraulic diffusivity as well as hydraulic conductivity of the uppermost sandy layer.

The properties used in this model:

Storativity	0.2
Hydraulic conductivity (m/d)	600
Aquifer thickness (m)	3
Transmissivity (m^2/d)	1800
Hydraulic diffusivity (m^2/d)	9000
Number of nodes	270
Δx (m)	5
Number of time steps	689
Interval of time (d)	1

Table 16: Parameters used in the one-dimensional numerical model

Figure 20 presents computed and observed data for wells w8 to w1 as well as river stage (dashed lines). The model was run from 07/28/2010 to 06/17/2012. As can be seen, river stage has an important effect on simulated groundwater-table fluctuations in all the wells. The water levels in wells w8 to w7, closest to the river, closely match the river stage. Wells from w6 to w1 have a similar pattern with the river stage. But, unlike w8 to w7, the patterns have been slightly changed. The amplitude of water table fluctuation is damped by up to 0.2 m, and the phase is lagged by about 50 days in the wells furthest from the Rio Grande (w1 and w2). The further the well is from the river, the smaller amplitude of the water table fluctuation in the well, and the bigger the phase

lag. The difference between the observed and computed water table for the 8 wells may be influenced by the spatially varying transmissivity, which was not considered in this model. At certain periods of time (approximately days from 0 to 200, days from 360 to 600 (August, 2010 to Feb, 2011 and September, 2011 to February, 2012)), the observed groundwater table have lower levels than the simulated ones. This may result from the interpolation errors of the Rio Grande stage or the underground aquifer discharge. In well w1, the observed groundwater table is slightly higher; there might be a small amount of groundwater recharge to w1 from the adjacent upland hills.

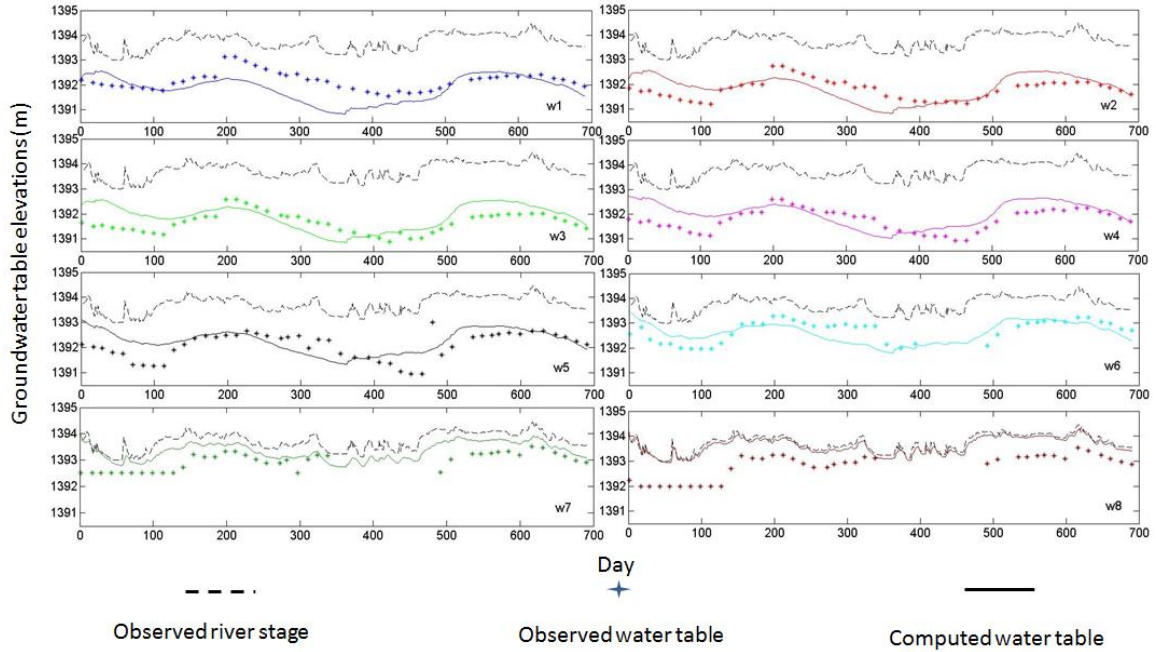


Figure 20: Numerical model in MATLAB loosely based on Rorabaugh's equation

River stage is an important factor effecting the groundwater table elevations in the field. By dropping 0.5 m in the river stage, the simulated groundwater table drops down by approximately 0.5 m in each well (Figure 21). For wells closer to the river, the simulated water table is more sensitive to the river stage changes. For wells further from the river, longer time the simulated water table levels take to change in response to river stage fluctuations. Shifting the river stage had no effect on the amplitude and phase lag in each well. This is because that the aquifer properties have not changed.

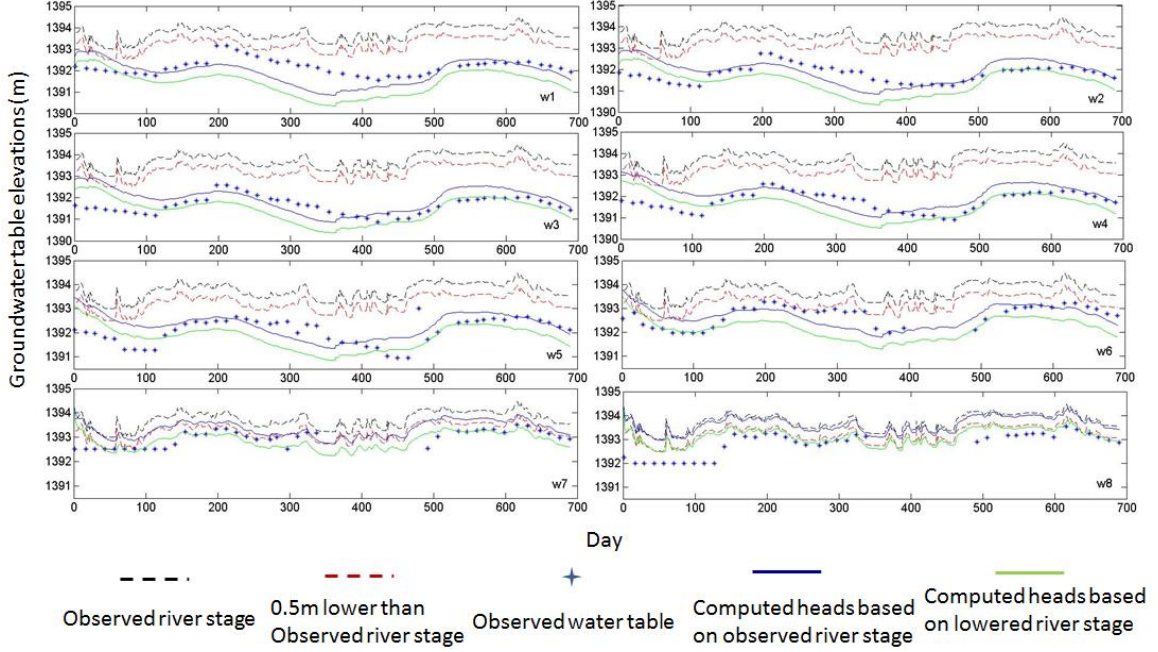


Figure 21: Effect of river stage on simulated groundwater tables by dropping 0.5m

Next, we considered the effects of hydraulic diffusivity on simulated head changes (Figure 22). The dashed line is the river stage, star is the observed head in the wells. The three other curves are the computed heads based on different values of hydraulic diffusivity $\frac{T}{S}$ ratios. Green curve is the computed heads using the best-fit hydraulic diffusivity $\frac{T}{S}$, blue curve is for a model run using a hydraulic diffusivity 10 times bigger ratio, and red curve is for a model run using a hydraulic diffusivity 10 times smaller. The hydraulic diffusivity and the distance from well to river determine the amplitude and phase lag of the water table elevations in wells. Bigger diffusivity result in simulated water levels closely resembling river stage. The groundwater tables are more likely to be affected by the river, (e.g., When increase the hydraulic diffusivity by 10 times ($\frac{T}{S} \times 10$), the phase lag in wells is about 5 to 10 days shorter, the amplitude becomes closer to river stage amplitude.) .Spatially, wells closer to the river (x is smaller) have closer trends to the river.

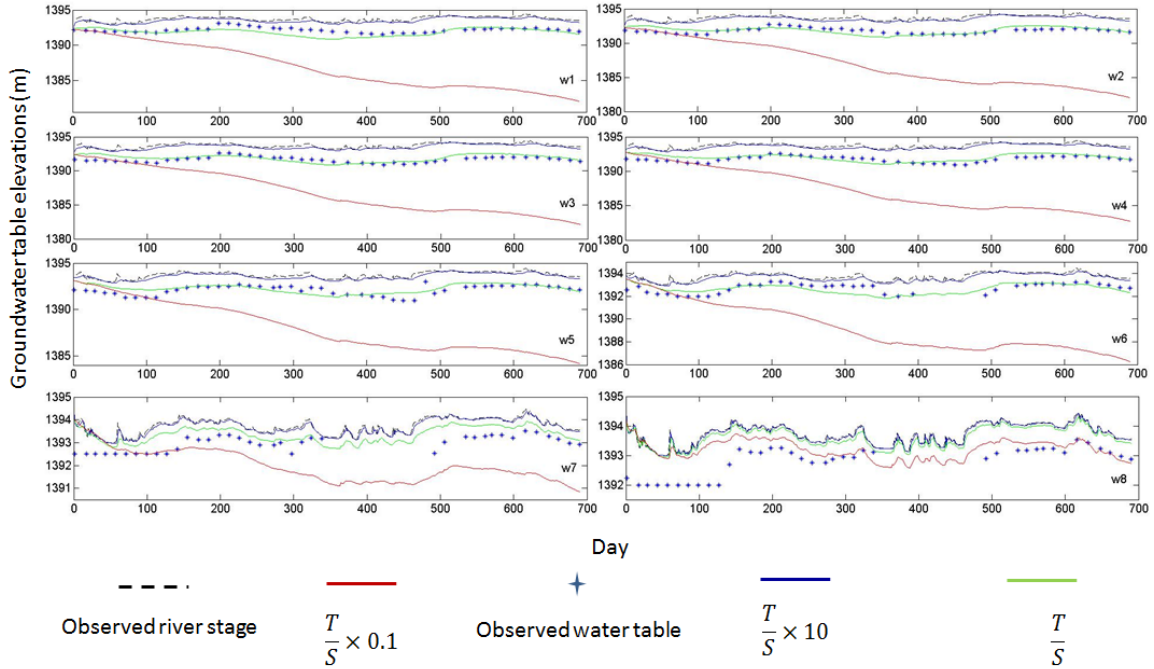


Figure 22: Effect of hydraulic diffusivity on groundwater tables by decreasing/increasing by 10 times

Finally, the simulated groundwater table is also influenced by the changes in strength of source/sink term ($R(t)$) (Figure 23). The influences of $R(t)$ is strongest for wells furthest from the river. Wells close to the river are not influenced by changes to $R(t)$ (w8 to w7). Water table changes in w1 which is furthest from the Rio Grande have approximately 0.5 meter changes, while the water table in w8 which is closest to the river has almost no changes when changing $R(t)$ by 0.001m at every day. When comparing the changes made by the hydraulic diffusivity with the changes made by $R(t)$ term, the effect of changing $R(t)$ is much weaker.

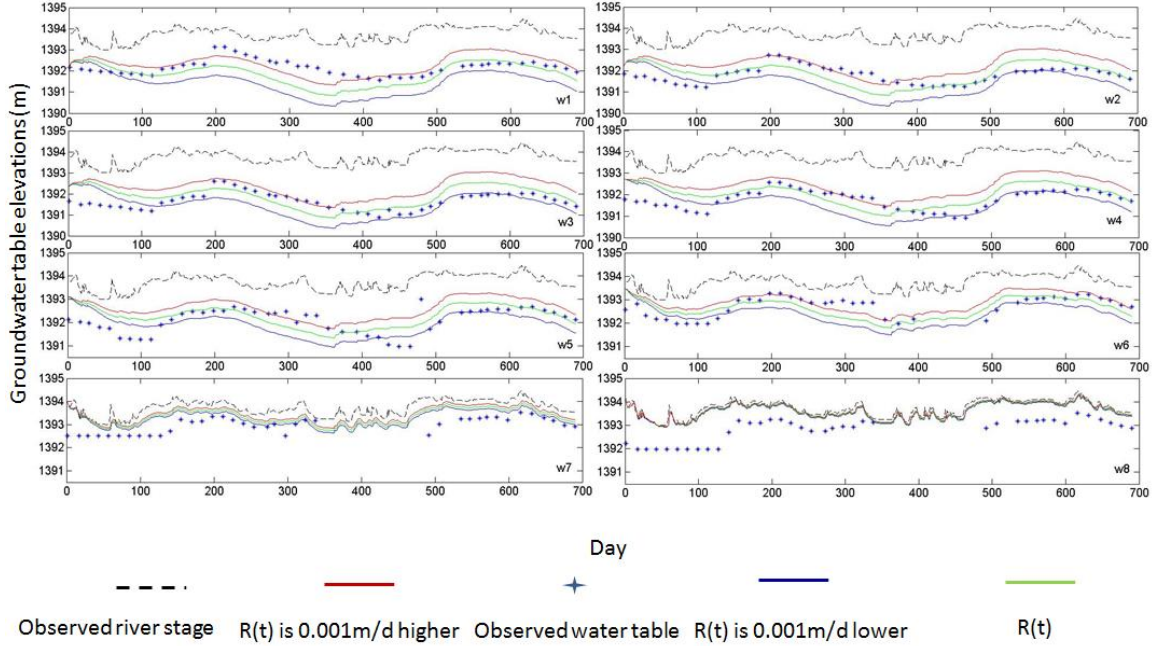


Figure 23: Effect of the magnitude of the source/sink term ($R(t)$) on simulated groundwater tables by decreasing/increasing 0.001m every day

4.6 Three-Dimensional MODFLOW Results

The one-dimensional analysis presents above provides insights into the influence of river stage, hydraulic diffusivity and the source/sink term on water level fluctuations within the study area. However, the one-dimensional model doesn't account for the effect of river channel sinuosity nor the down-valley groundwater flow on water-table elevations. The Rorabaugh analysis also does not account for vertical leakage across different stratigraphic layers. In addition, spatial variation in evapotranspiration, precipitation, hydraulic conductivities, as well as human impacts, such as draining, pumping and irrigation, also influenced the groundwater table in this region. A three-dimensional model is needed to assess the influences of all of these other factors.

We present both steady state and transient three-dimensional numerical models of groundwater flow and water table fluctuations within the Bosquecito study area using MODFLOW. We used this model to further assess the influential factors controlling water table fluctuations within the wetland. We also used this model to delineate the potential extent for wetland hydrology.

4.6.1 Steady State MODFLOW Model

We constructed a four-layer MODFLOW model to represent hydrologic condition within the Bosquecito wetland near San Antonio (Figure 5). Our model includes a relatively low permeability layer at the soil surface which is primarily composed of silt and clay. Below this layer, we included a relatively high permeability sandy layer (Layer

2), a second low-permeability confining layer (layer 3), and a basal aquifer having a high permeability (layer 4) which is composed of gravel and coarse sand. The hydraulic conductivity for each layer was adjusted from the reference data for different materials (Bear, 1972, Freeze & Cherry, 1979, Schulze-Makuch et al, 1999). Specific storage used in this model was taken from the hydrograph analysis presented in section 4.1. Specific yield is from experimental data (Johnson, 1967). The pumping rates used in layer4 for the wells on the west side of San Antonio are the average ($587 \text{ m}^3/\text{d}$) for the study period. The LFCC is specified to the west of the Rio Grande. It proved to be a very influential factor for groundwater tables in this region. Elevations of the LFCC come from the survey and DEM (Figure 16, Richards, 2006); and the LFCC's conductivity is adjusted from reference data (Richards, 2006). The ETS package was used in this model. The maximum ET used is the average ET from the RAWS station results from the Kimberly-Penman calculation during the study period. The extinction depth for the MODFLOW ETS module is assigned to be 3 m. Localized ET is also applied in high ET areas on the wetland side, based on the NDVI map during a one year duration. Precipitation is from the RAWS station observation data. For the specified flux on the north boundary of the research domain, the injection rate for each cell is set as $50 \text{ m}^3/\text{d}$. Recharge for the west side of this research site is computed from the balance between irrigation (positive), precipitation (positive) and evapotranspiration (negative). Negative recharge is set to be 0. Recharge for the east side of the research site is computed from the balance between precipitation (positive) and evapotranspiration (negative). Negative recharge is set to be 0 as well. Recharge applied in the steady state model is averaged recharge over the study period on either side (Table 17).

Hydrostatic properties										
Layer number	Horizontal K (m/d)	Vertical anisotropy	Thickness (m)	Specific storage (1/m)	Specific yield	Porosity				
Layer1	7	4	3	5×10^{-6}	0.1	0.3				
Layer2	220	2	6	5×10^{-6}	0.2	0.3				
Layer3	20	3	1	5×10^{-6}	0.1	0.3				
Layer4	150	2	14	5×10^{-6}	0.2	0.4				
LFCC										
Bottom elevation of the north boundary m	Bottom elevation of the south boundary m			Conductivity m/d						
1390	1387			1						
ET										
ETSS elevation	Maximum ET m/d		ETS extinction depth m		Extra ET m/d					
Various with the land surface elevation	0.004		3		0.002					
Recharge										
West side recharge rate m/d	East side recharge rate m/d									
0.0005	0.0004									
River										
River bed elevation north m	River bed elevation south m									
1394	1391									
River water table elevation at north boundary	River water table elevation at south boundary									
1395	1392									

Table 17: MODFLOW parameters and boundary conditions used in the steady state three-dimensional model.

Observed water table in wells come from the average of the water table measured in wells w1-w8 during the study period. The simulation result of the water table in wells gives a relatively close match to the observed heads data (Figure 24). Total observation head variation is 1.4 m, computed heads variation is 1.25 m, the errors between the computed heads and observed heads are between 0.02 m and 0.4 m.

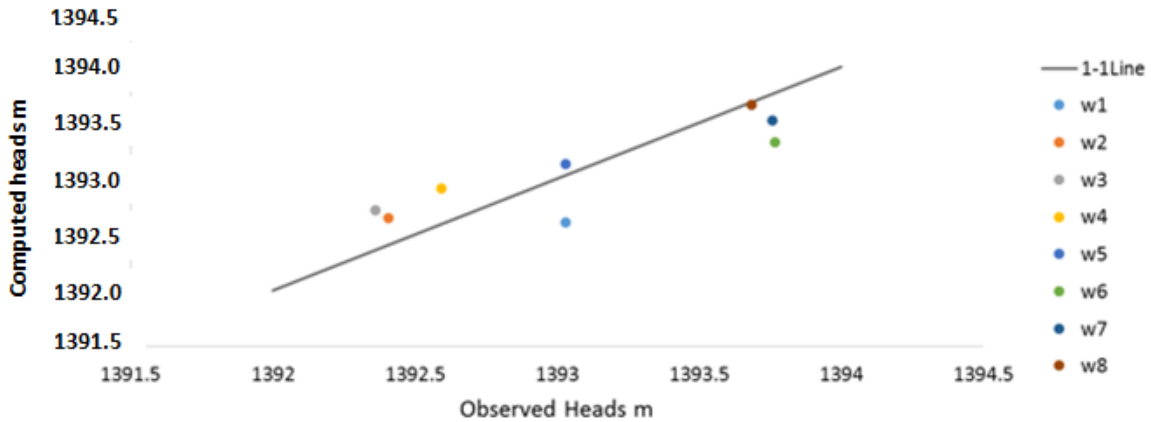


Figure 24: Observed data versus best fit computed heads data from model calibration

Figure 25 shows the groundwater contours in this site from observed and simulated data, color blue is the computed data from the model, color orange is the observed data from Anderholm's report. The computed data is very close to the observed data, maximum difference is 1.23, and smallest difference is 0.64. It is reasonable to believe the simulated groundwater contours are close to the true groundwater contours.

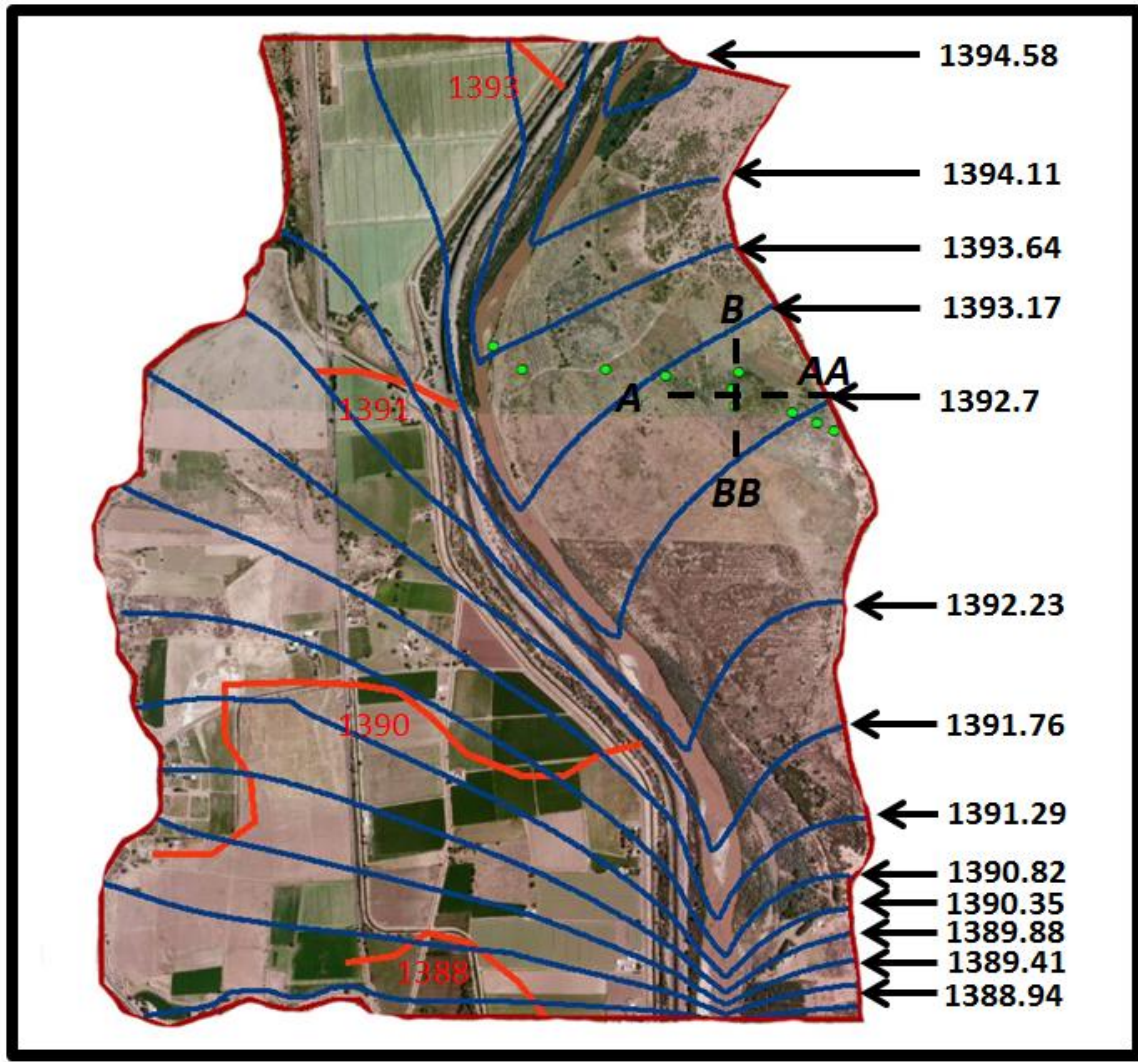


Figure 25: Comparison of steady-state computed heads contour to published water-table map. (Orange: observed heads (Anderholm 1987), Blue: Computed heads (m) exported from MODFLOW model with interval 0.47m)

Based on the simulated contours map of the groundwater table, the heads at the north, south, east and west boundaries are reported in Table 18. The heads measured to the north and south of well w4 in wells N04 and S04 are reported in Table 18 as well. These wells are 148 m apart. To compute the east-west gradient, we used average heads from wells w1 and w5 (Table 18).

The hydraulic gradient is calculated using equation below:

$$i = \frac{dh}{dl} \quad (4.2)$$

where i is hydraulic gradient, dh is heads difference, dl is the distance between two locations.

Location	A	AA	B	BB
Heads m	1393.12	1392.78	1393.17	1392.7
Distance m		720.52		540
Well	w5	w1	N04	SO4
Heads m	1399.665	1399.272	1399.703	1399.556
Distance m		720.52		139.87

Table 18: Heads at each locations and their distances

Based on the equation (4.2), the hydraulic gradient calculation is shown as below

	Hydraulic gradient based on observed data	Hydraulic gradient based on computed data
north to south direction	0.001	0.0009
west to east direction	0.00048	0.00047

Table 19: Observed and simulated hydraulic gradients on two directions

Hydraulic gradient calculated from the computed data on north to south direction is slightly smaller than the observed one (Table 19). Normalized error percentage is 10%. Hydraulic gradient on west to east direction based on computed data is also smaller than the observed one. Normalized error percentage is 2%. Errors may result from permeability heterogeneity within the aquifer, river bed conductivity variations at different locations on the river in this model, etc. Other factors, such as spatial ET rate variation, aquifer leakage and recharge, may also contribute to these hydraulic gradients differences.

The model receives water from the northern boundary inflow, precipitation and the river. Water leaves the domain across the downstream (southern) boundary and the drain (LFCC). In the steady-state model result, a large areas of the model in the first layer is dry, small areas in layer 2 are dry, while layer 3 and layer 4 are fully saturated. Water table contours in different layers are almost identical. Except for the water table on the west side, where the extraction wells are located. The water table varies only slightly in layer4. Computed head patterns indicate that the river water recharges the shallow aquifer (Figure 25). This proves to be the main source of water for the wetland. The river stage, as well as riverbed conductivity, are also potentially important factors controlling the groundwater-table elevations within the study area. The LFCC drains about 30% of the river water that leaks into our model domain from the Rio Grande (Table 20), and alters the groundwater flow directions. ET within the study area consumes about 20% of the Rio Grande water that leaks into the model domain, driving groundwater flow away from the river (Figure 25). It lowers the groundwater table in the vicinity of the wells w1 to

w5. Wells (w8, w7), closer to the river, are more influenced by river and LFCC, while the wells (w5 to w1), further to the river, are more strongly affected by the ET and regional ET.

Unit: m^3	Flow in	Flow out
Sources/Sinks		
Constant head	0	-39224
Wells	0	-3522
Drains	0	-33967
River leakage	95454	0
Recharge	4374	-2532
ET segments	0	-20584
Total sources/sinks	99828	-99828

Table 20: Flow budget of the steady-state model

From the steady-state model budget (Table 20), the river leakage is 5 times greater than total ET, but only 3 times greater than LFCC drain inflow. This means the LFCC greatly influenced the groundwater tables, while the influence of ET is a secondary factor.

4.6.2 Transient Model in MODFLOW

In the transient model, properties of the soil layers were the same as in the steady-state model. River properties are all the same. LFCC was assigned a hydraulic conductivity of 3 m/d in the transient MODFLOW model. Pumping was specified between June to November. The pumping rate applied in this model was taken from the Blaney-Criddle water demand estimates. Maximum ET is the average ET during the study period from RAWS station in Bosque del Apache and applied each day. Extinction depth is 3 meters. Regional ET is applied in high ET regions by -0.001m/d discharge in the first layer. Transient recharge for the west side of the research domain is from the summation of the precipitation (positive), irrigation (positive) and evapotranspiration (negative). The negative recharge is set to be zero. For the east side, it is the summation of precipitation (positive) and evapotranspiration (negative). Negative recharge is set to be 0 as well. The recharge is different from the 1D transient model, in which pumping is not considered. The river stage, the LFCC properties, layer3 properties, human impacts, the ETS package, and the regional ET for the site are tested for their sensitivities for this model.

After running the 3D transient model, the results are shown in Figure 26:

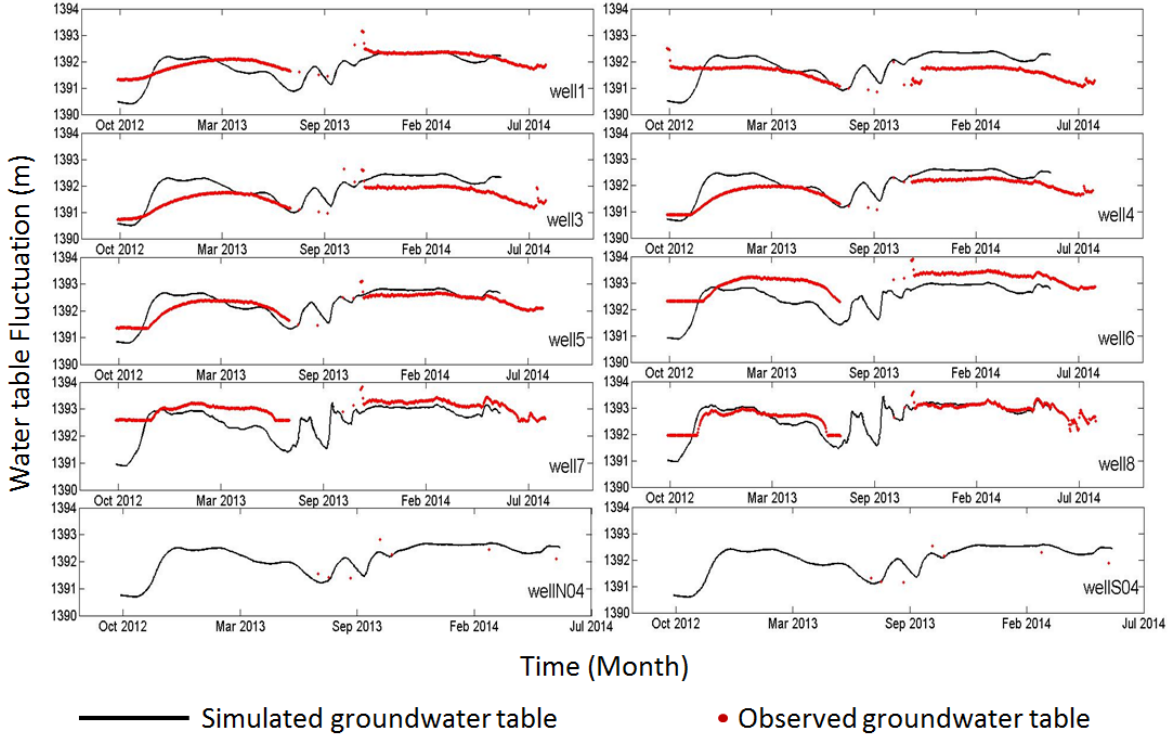


Figure 26: Comparison of observed and simulated groundwater table from transient MODFLOW model.

The 3D simulation period starts from October 2012 to June 2014. The computed heads are very similar to the observed heads. Both in observed and computed results, groundwater tables in well w8 and w7 show a strong correlation with the river stage. They are the wells nearest to the Rio Grande. From wells w6 to w1, the groundwater table is less affected by the river stage fluctuations. Other factors such as regional evapotranspiration, spatially changing aquifer properties, groundwater/surface-water interactions may have a second-order impact in determining groundwater-table fluctuations in this area, and become relatively more important as the distance to river becomes longer.

This 3D model considers many influential factors for the groundwater fluctuations. It is a much more complex model than the 1D transient model. This model has vertical and horizontal groundwater flow in 3D. Many other factors, such as layer effects, drain, ET, regional ET, pumping/irrigation are all incorporated in the model.

Unit: m^3	Flow in	Flow out
Sources/Sinks		
Storage	1877	-184
Constant head	1272	-5574
Wells	0	-7200
Drains	0	-37344
River leakage	51205	0
Recharge	0	-1647
ET segments	0	-2426
Total sources/sinks	54355	-54376

Table 21: Flow budget of the transient model

In the transient model, ET takes about 5% of the river leakage, which is smaller than the percentage of the ET relative to river leakage in the steady-state model. This may be due to the influence of the ET extinction depth and the groundwater fluctuation. The river leakage is 1.4 times greater than the LFCC drain, it is because the hydraulic conductivity of the LFCC in the transient model is slightly bigger than that of the steady-state model's.

4.6.3 Sensitivity Analysis

There are considerable uncertainties in aquifer parameters and hydrological stresses in the model of this study area. We conducted a sensitivity analysis to further test which factors had the largest effects on water table levels for this site. In the analysis, river stage, riverbed conductivity, LFCC conductivity, pumping rate, layer3 properties, maximum ET, and the regional ET are tested to find out their influences.

4.6.3.1 Rio Grande Stage

The river stage has the largest impact on simulated groundwater table in these wells. The influence is manifested in the observed data, and discussed in the 1D model and the 3D MODFLOW simulations above. When decreasing the river stage by 0.2 m, the groundwater table in wells drops by around 1 meter at the largest change in a specific period. This may be due to a variety of reasons. By checking the hydraulic conductivity of the river, most likely, it is because the small flow rate (low hydraulic conductivity 7m/d) from the river to its riparian, when the river stage drops, less water is available from river to replenish the water consumed by ET in the riparian lands. The wells are closer to the river, the bigger the faster the changes in the groundwater fluctuations. When the river stage becomes relatively stable, the water table in wells also tends to be stable, but the wells near the river become stable faster.

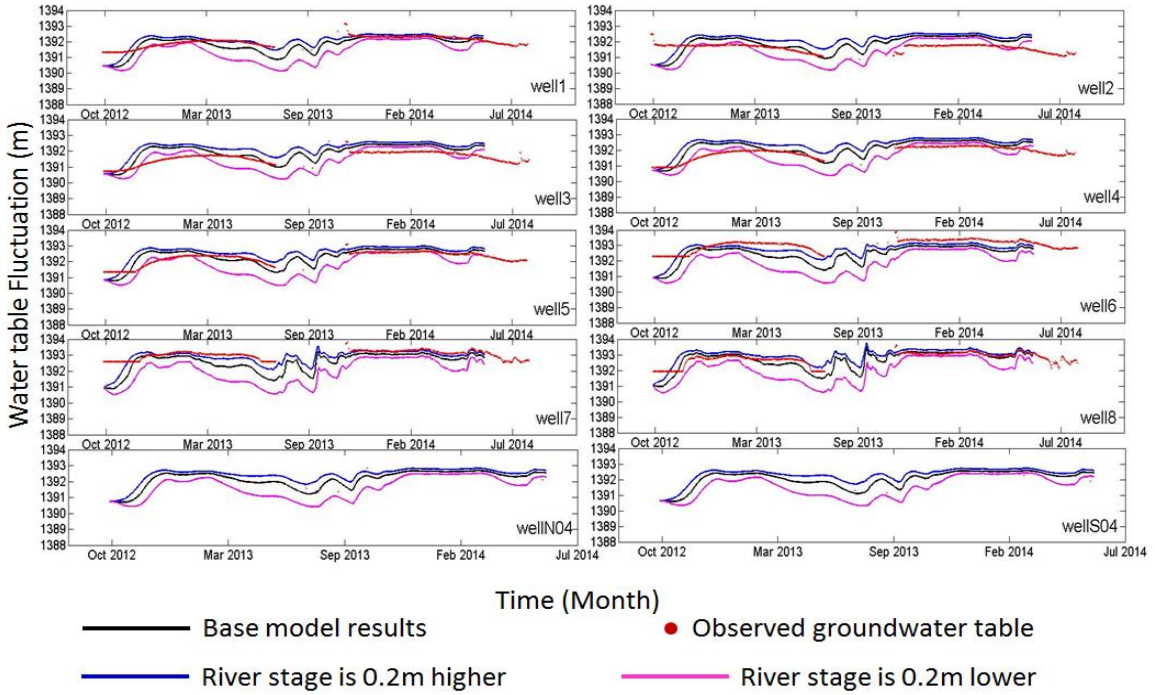


Figure 27: Effect of change in river stage ($\pm 0.2\text{m}$) on simulated water table elevations

4.6.3.2 Riverbed Conductivity

The river bed conductivity determines the volume of water that infiltrates from the river into the top layers of the model, which affects the groundwater tables. For the base run, the riverbed conductivity was set at 7 m/d. A decrease in riverbed conductivity by 1m/d results in around a 0.5 m changes in the groundwater table in well w8 (Figure 28). Wells closer to river are more likely to be affected by the river, having bigger changes. When the river stage becomes stable, wells closer to the river stabilizes first. When increasing riverbed conductivity, the groundwater table is higher, and more closely resembles river stage.

Decreasing the riverbed conductivity resulted in smaller water table changes in each well. Smaller river bed conductivity will permit less water to recharge the aquifers per unit of time, making the groundwater table lower. A larger river bed conductivity means more surface water enters the aquifer. River bed conductivity controls the amount of river losses and directly changes the groundwater table at this site.

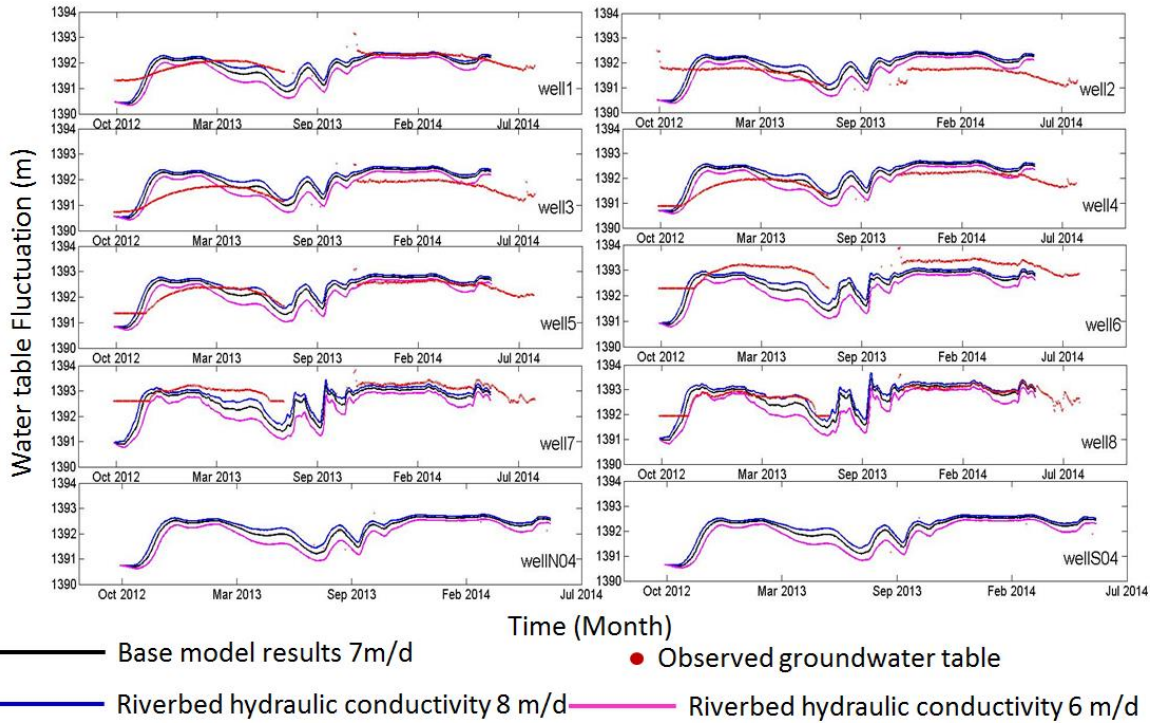


Figure 28: Effect of change in riverbed conductivity on simulated water levels

4.6.3.3 LFCC Conductivity

LFCC is located on the west side of the river bank. The LFCC also strongly affects the simulated groundwater tables in the study site on the east and west sides. The LFCC is a drainage system that not only collects the excessive surface water (Shafike, 2004) from the irrigation land, but also acts as a groundwater drain. The LFCC is designed to be 5.2 meter lower than the river bed, making it a large regional drain system. The higher the drain conductivity, the more water from aquifer is captured. Groundwater wells closer to the river (close to the drain) are more likely to be affected by the drainage. The drain conductance was set to be 3 m/d, as shown in Figure 29, a 1 m/d change in the LFCC conductivity results in around 0.5 m change at most in the groundwater table in these monitoring wells near the river (w7, w8).

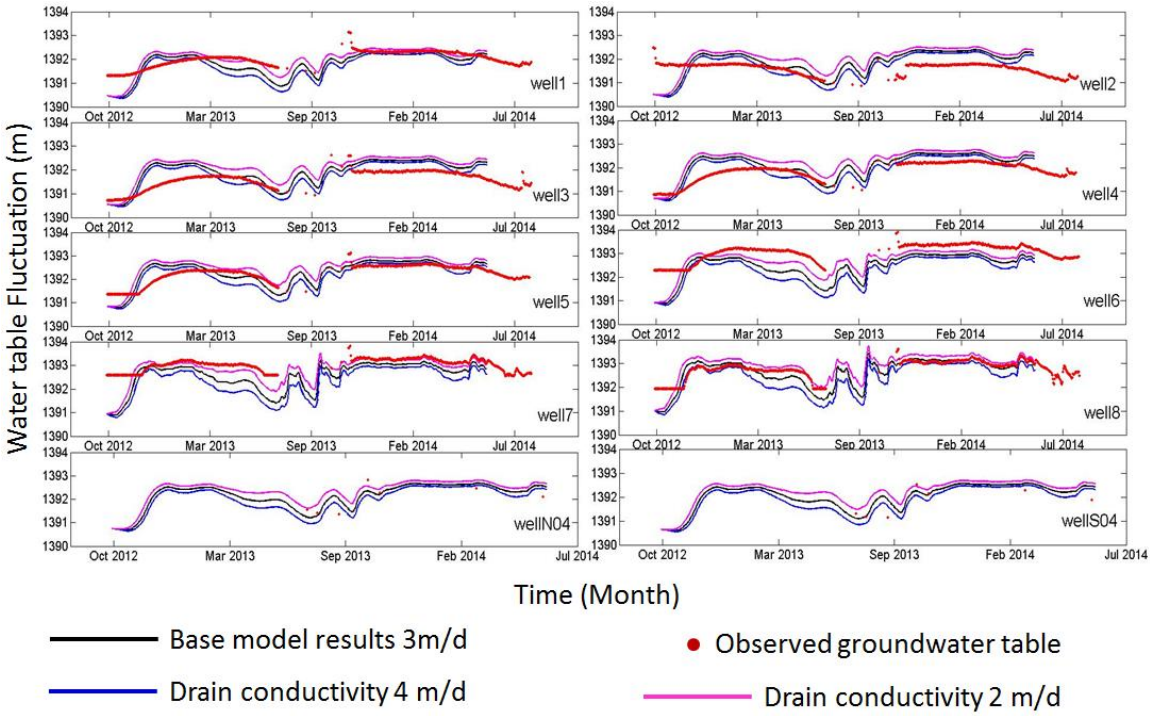


Figure 29: Effect of change in drain conductivity ($\pm 2\text{m/d}$) on simulated water table elevations

4.6.3.4 Pumping and Confining Unit

Layer3 in our model has a low hydraulic conductivity. This is consistent with a prior groundwater model for this area (SSP&A, 2003). The low hydraulic conductivity layer is believed to be a confining unit between the layer2 and layer4 (Richards, 2006). All the irrigation wells in our model are screened in layer4, so water for the wells is from the fourth layer. Because of the low permeability layer3, we hypothesize that pumping activities won't influence the groundwater tables in layer2 and layer1 significantly. In addition, the excessive irrigation water applied on the surface on the west side of the model domain is influenced by the LFCC drain, making the influence from irrigation smaller on the east side of the model domain. From Figure 30, comparing the pink curve with the black curve, groundwater table is almost the same. This demonstrates that the low hydraulic conductivity layer3 damped the effect on the simulated water table on the east of the Rio Grande in the wetland from the west side pumping and irrigation. Comparing the blue and pink curves, by keeping the pumping rate constantly high, and letting the hydraulic conductivity of layer3 equal layer4 (150 m/d), the groundwater table still does not significantly change. This suggests that the distance from pumping wells to the monitoring wells is great enough to diminish the influences from pumping on the wetland.

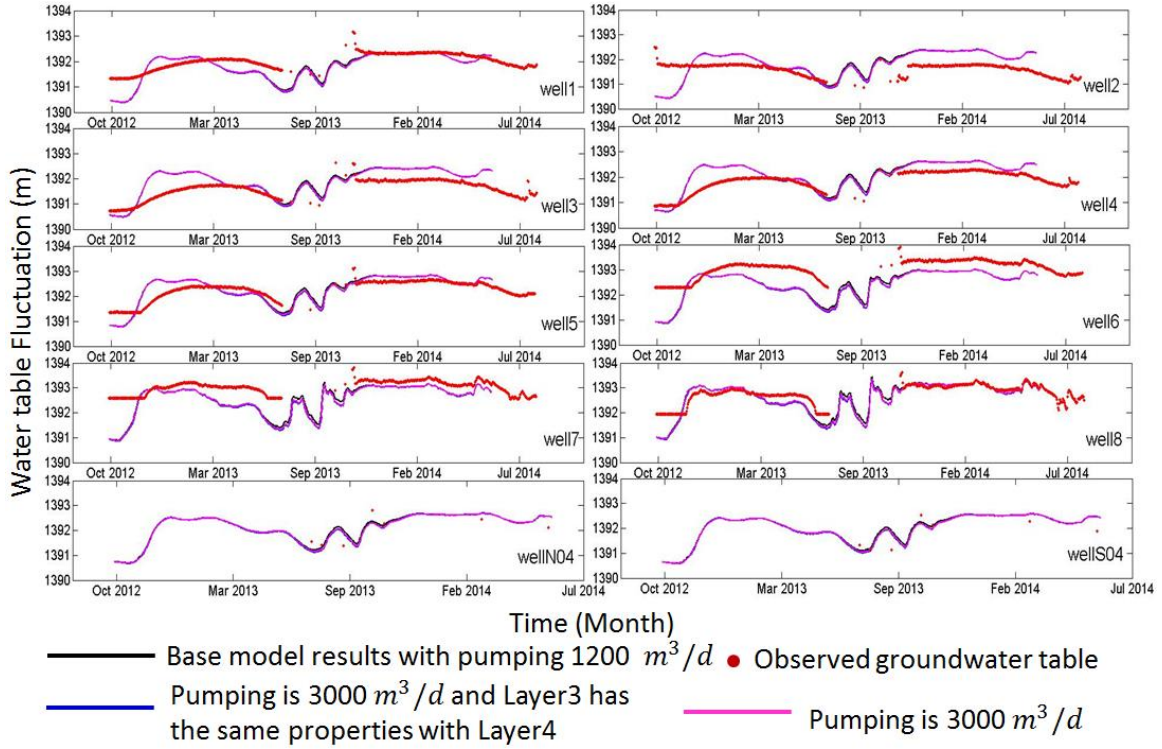


Figure 30: Effects of pumping rate and the confining unit (Layer3) on water table elevations

4.6.3.5 ET Effects

Evapotranspiration was applied using ETS package. We found that it slightly affects simulated water tables when compared with the effect of river. Maximum ET used in the ETS package of this model is 0.004 m/d, the averaged ET value from the RAWS station data over the study period, and the extinction depth in model is 3 m. The ET rate linearly decreases until it reaches the extinction depth at 3 m. By using ET 0.002 m/d and 0.006 m/d as maximum ET in this model to test the ET effect, it shows that the ET is a secondary factor affecting the groundwater table in this area. Wells close to the river, well w8 and w7 are strongly controlled by Rio Grande, while the wells further to the river are more likely to be influenced by ET. The ET is increasingly influential with increasing distance to Rio Grande.

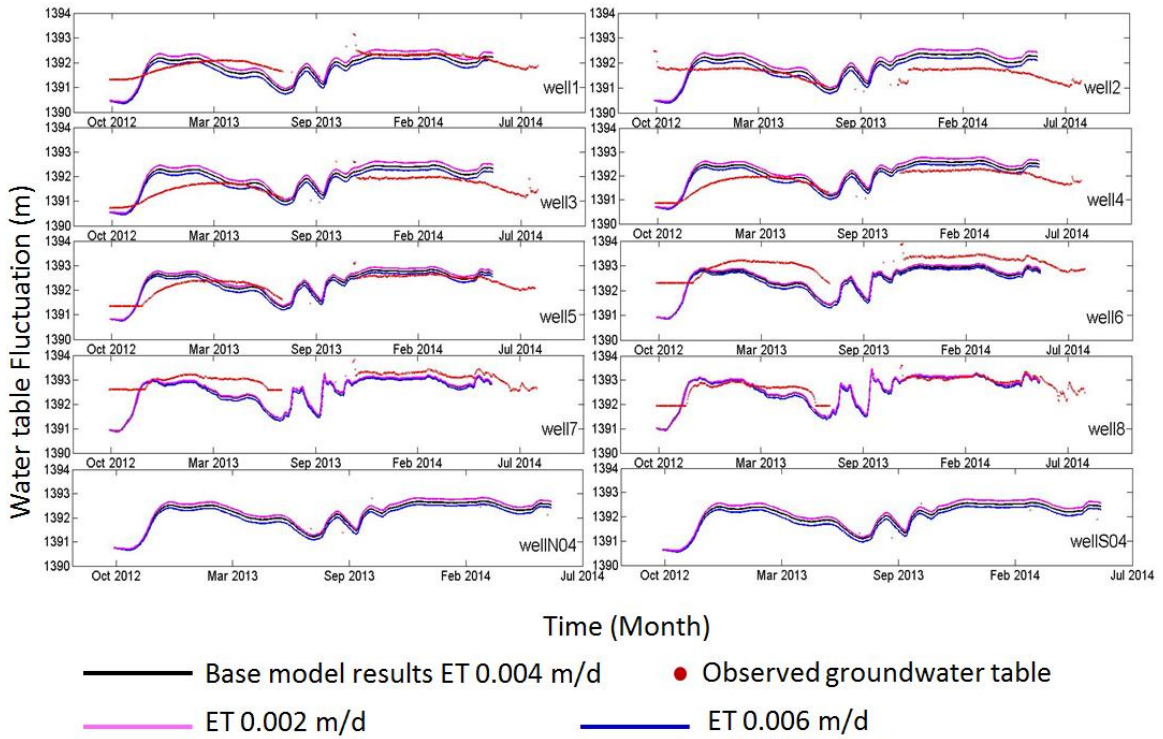


Figure 31: Effects of evapotranspiration on groundwater table changes

4.6.3.6 Regional ET Effects

Regional evapotranspiration also plays a role in the groundwater table fluctuations on the east side of the wetland (Figure 32). It is the area with the highest ET (evidenced by the NDVI analysis (Figure 19)). Changing regional ET slightly altered the groundwater flow directions, lowering the groundwater table in wells from w1 to w6 (Figure 32; Figure 33). But the groundwater table in w8, w7 shows only a small influence from the regional ET. They are the wells close to Rio Grande, having immediate river water recharge, strongly correlated with the river stage. Without regional ET, groundwater tables are higher in well w6 to w1 and the ponded area is bigger. (Figure 33)

To further confirm the regional ET effects, a test in the steady-state model is conducted and the results are shown in Figure 33.

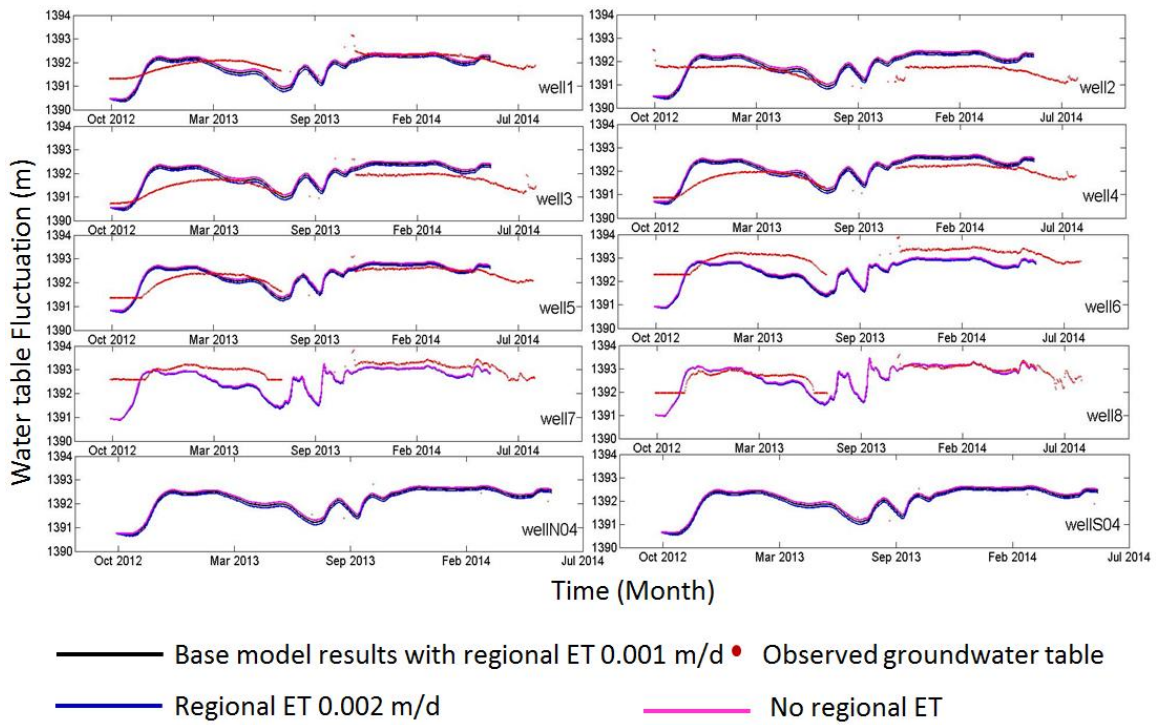


Figure 32: Regional ET changes effects in the transient 3D model

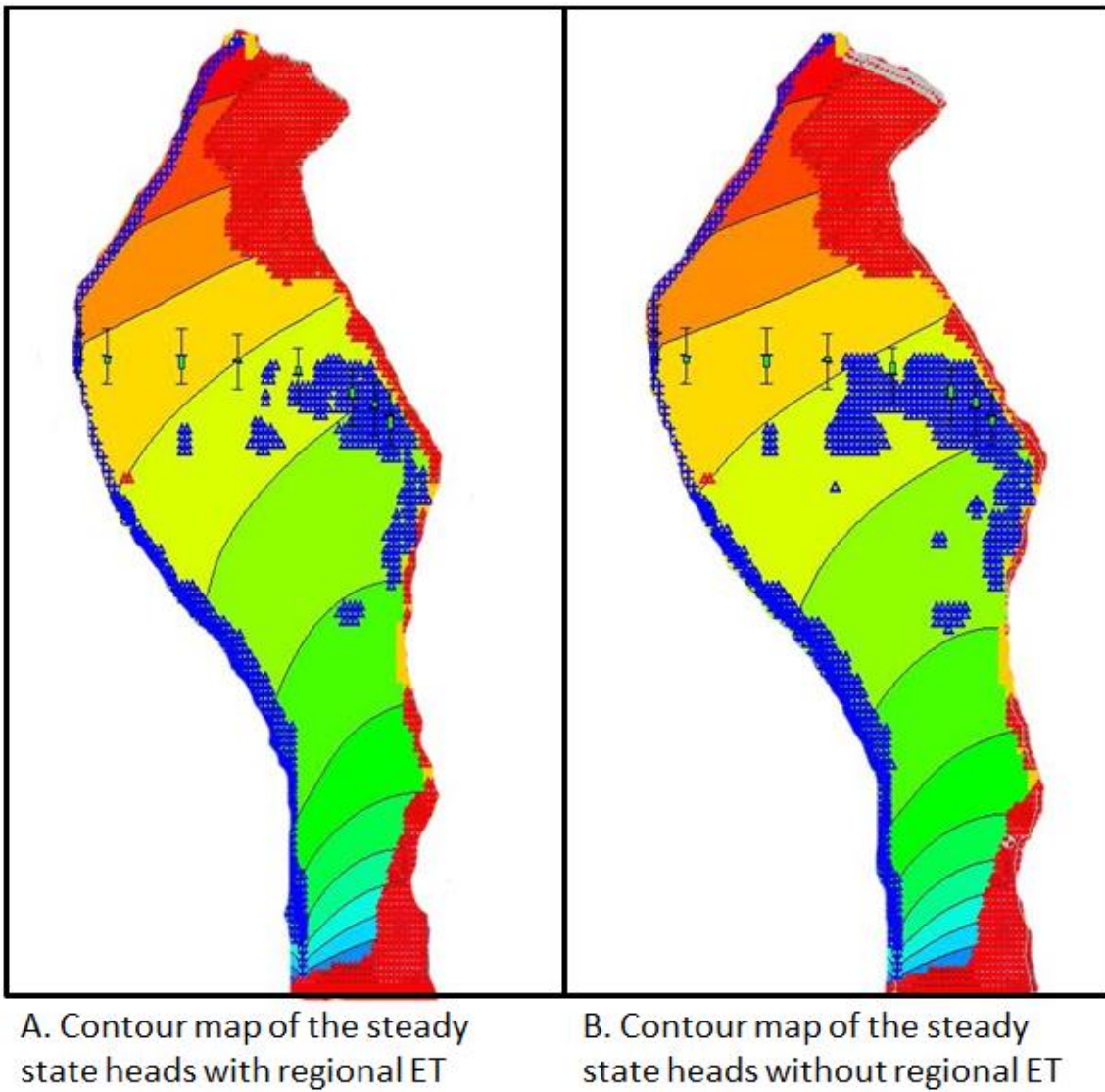


Figure 33: Contour map of the steady-state 3D model with/without regional ET (Red area is the place where the groundwater tables are below the first layer (3 m), blue area is the place where the groundwater table is above the land surface.)

4.7 Influential Factors for the Groundwater Tables in Wetland Side

As with the one dimensional model, using our three dimensional model, we found that the most important factors for the wetland's groundwater tables are the Rio Grande stage and riverbed hydraulic conductivity. The LFCC also changes the groundwater tables in wetland side by acting as a regional drain. They are the first-order influencing the water-table depth factors. ET for the whole area is also considered to be influential. Additionally, in the wetland side, the groundwater tables are slightly altered by the regional ET in high-ET regions, based on the Landsat image analysis. They are the second-order factors. The first-order factors strongly affect the groundwater tables in the

wetland side, while the second-order factors exert their impacts on the wells more distant from the river.

4.8 Hydric Soil and Wetland Delineation Using Simulated Water Table Fluctuation

The National Technical Committee for hydric soil defines a hydric soil as a soil that formed under conditions of saturation, flooding, or ponding long enough during the growing season to develop anaerobic conditions in the upper part (Vasilas et al, 2010).

The Hydric Soil Technical Standard states that for a soil to meet the definition of 'hydric', the water table must be within one foot of the soil surface for 14 consecutive days during growing season in a normal or drier precipitation year (National Technical Committee for Hydric Soils, 2007).

Growing season in Albuquerque is from April 6th to November 6th (Malone & Williams, 2010). Based on the simulated transient groundwater table data for 2013 and the land surface elevation, we built a transient model and ran it in MATLAB. The transient model operates on a time step of one day, and the wetland size expands and shrinks every day, but never goes extinct.

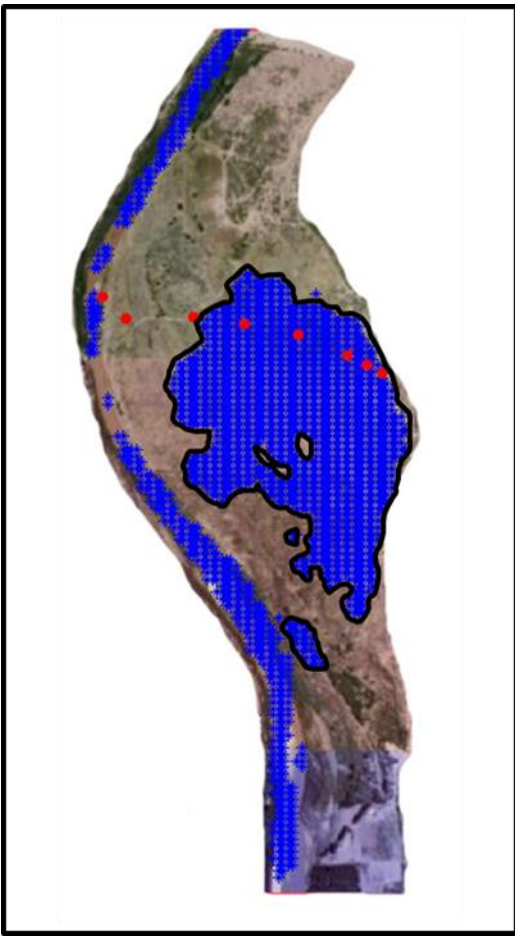


Figure 34: Delineated wetland boundary based on 2013 data and the HSTS condition

Based on the model, the wetland on the east side of the bank is calculated and shown as the blue area delineated with black curves in Figure 34.

CHAPTER 5

DISCUSSION

5.1 Testing of Model Results

5.1.1 Surface Water and Dry Area

Using average hydrologic stress conditions and best-fit model parameters, the calculated water table from our 3D steady state numerical model in MODFLOW intersects the land surface in the vicinity of the wetland (Blue areas in Figure 35A). The area where the water table is at the land surface is consistent with Landsat images collected from the study area. Figure 35B and C present two NDVI maps of this study site in September and October. In Figure 35B and C, black color in the NDVI pictures represents negative NDVI, where surface water rests. Other colors represent different NDVI value ranges (Different ET rates) (Table 10). Blue stands for the highest ET region; pink is the area of lowest ET. In the modeling results (Figure 35A), the red is the region where the water table drops below the bottom of the first layer of the model, which is 3 m below land surface.

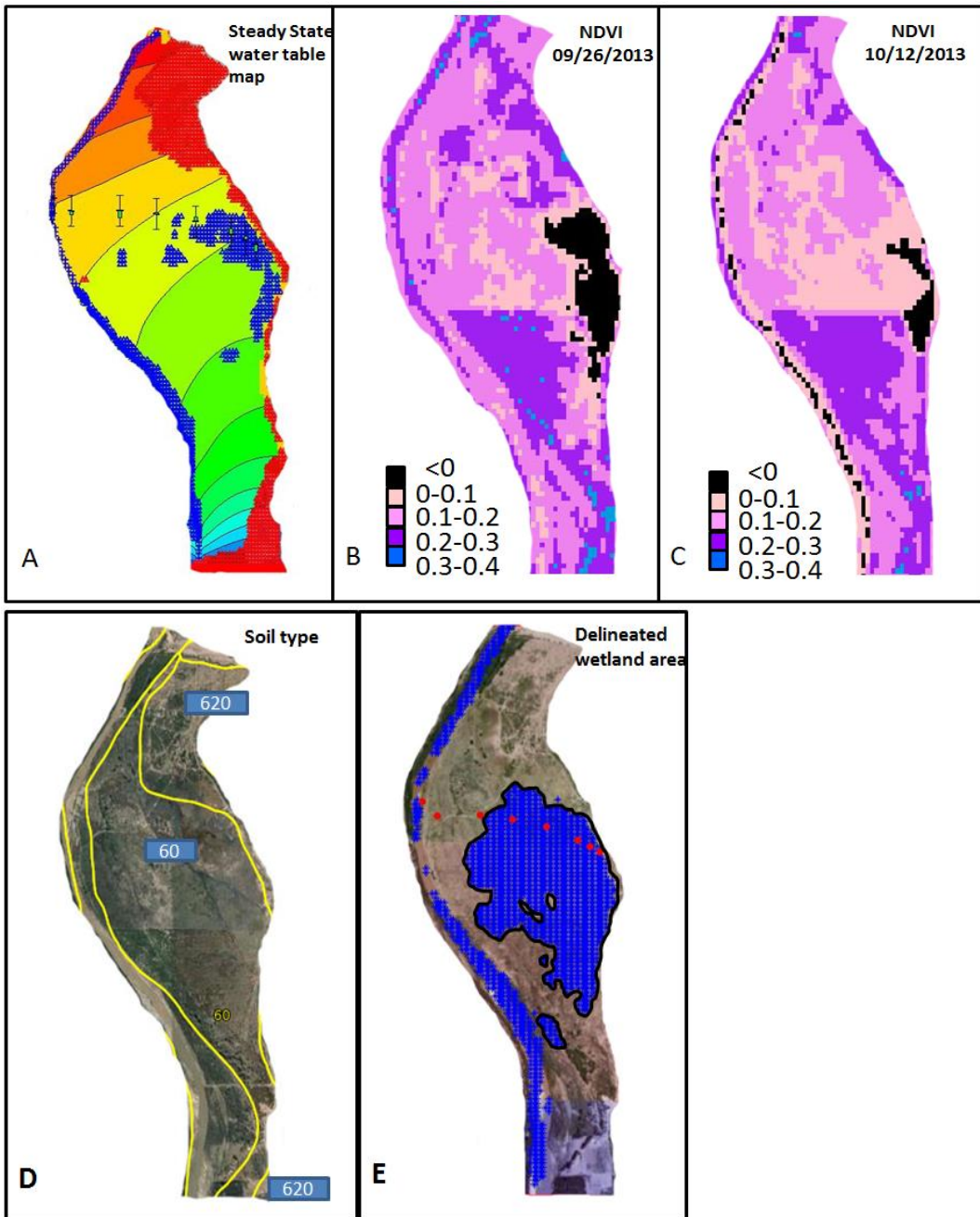


Figure 35: (A) Comparison of the calculated steady-state flooded (Blue) and dry (Red) area with observed information; (B) (C) NDVI images of 09/26/2013 and 10/12/2013; (D) Soil type, see Table 5-1 for soil properties description; (E) Wetland delineation based on transient model results, blue areas enclosed with black curves are the proposed wetland areas.

Figure 35D shows different types of soils and their distribution in this site. Different numbers represent different soil types. The yellow curves are the boundary of

soil types. Different soil types have different general drainage ability and water table depth (Table 22).

Soil type number	620	60
Name of the soil	Bluepoint loamy fine sand, 1 to 9 percent slopes	Typic Ustifluvents, 0 to 2 percent slopes
National map unit symbol	2sy14	1xg8
Natural drainage class	Somewhat excessively drained	Well drained
Depth to water	More than 80 inches	About 42 to 72 inches

Table 22: Soil distributions and properties (Soil data is from NRCS SSURGO dataset)

The soil types (as mapped by NRCS) in this study area suggest the relative groundwater table difference and the dry cells distribution. According to Table 22, the area where soil map unit 620 should have deeper groundwater tables, upland conditions would probably exist. Soil map unit 60 has a shallower groundwater table. In the simulated results, the groundwater table drops below the first layer shown as the red region in the model (Figure 35A). Comparing Figure 35A and Figure 35D, the red area shown in the simulated groundwater table contours supported this soil distribution based on the groundwater tables. The red area located in the same locations with the similar shapes.

5.1.2 Comparison of the Simulated Water Table Elevations with Hydric Soil Data

A preliminary report by Aaron Miller of the NRCS in 2010 (Miller, 2011) assessed the spatial distribution of hydric soils by applying the Hydric Soil Indicators (Vasilas et al, 2010) to soil descriptions at each site, and by describing the sediment cores collected in wells w1 to w8.

As described in the report, hydric soils were found near wells w1 to w4. Hydric soils were absent near the cores from wells w6 to w8. We used the MODFLOW model output to determine the wetland extent. We used the criteria for hydric soil that the depth between the groundwater table and the land surface must be less than 1ft for 14 consecutive days during growing season in more than half of the observed years. Using this criteria, the hydric soil were found to exist in w1 to w5 (Figure 35E). Discrepancy between the observed hydric soil distribution and the computed result may come from the uncertainties of the aquifer properties used in the model. Also, errors in the computed water table could come from the observation and categorization of soil types in the field. In addition, hydrophytes are found in the area between wells w5 and w6. This could indicate that during certain periods of time, water saturated conditions could occur between w5 and w6.

Based on the simulated groundwater table in this site, areas from well w1 to w3 have water table rising above the land surface, developing some period of surface

ponding, as seen in the NDVI map, but also, the filed investigation performed by Aaron Miller in 2010 where he observed flooding in this area.

5.2 Advantage of Hydrological Modeling Approach to Wetland Delineation

There are many ways to delineate wetlands. In general, they are categorized as onsite method and offsite method. Onsite methods are more precise, but require a huge amount of work and resources, while the offsite methods are more economical, but it provides rough estimates of wetland area. In general, both methods should be combined to ensure accurate wetland delineations.

The hydrological modeling approach is a relatively cheap and reliable way to add confidence to wetland delineation. Groundwater table were recorded automatically every hour with pressure transducer/data loggers, which were used in the model calibration. Field work and data analysis were used to test the hydrological properties. The hydrologic model results can be used to drive additional data collection. Additional wells could be drilled in areas where the model predicted shallow water table.

5.3 Conclusion

Water level fluctuations from a transect of wells across the Bosquecito, NM wetland suggests that the wetland in this semiarid region is mostly controlled by the river stage. The Rio Grande in this area is a losing river. In this study, we constructed simple 1D and 3D models of the Bosquecito wetland situated between Socorro and San Antonio, NM. Both the 1D and the 3D numerical models supported the hypothesis. During periods of high river stage or after the heavy rainfall events, groundwater rises to the land surface.

The LFCC which is 5.2 m lower than the riverbed also had an important effect on groundwater table fluctuations; water from Rio Grande goes into it via groundwater flow. The LFCC strongly impacts the stage of Rio Grande, which consequently affects the groundwater table in wetland side.

ET for the whole area affects the groundwater table elevations. Areas further from Rio Grande are more likely to have ET effects. Regional ET distribution plays a role in determining the groundwater flow direction in the aquifer and lowers the groundwater table in the high ET regions. The regional ET only affects the groundwater tables in places far away from the river as well. At wells w8 and w7, which are near to the river, the groundwater table is mostly determined by the river stage. Neither ET nor regional ET effects was observed in these wells.

Irrigation and pumping in the west side do not affect the groundwater table on the east side where the wetland is located. This results from the lower permeability layer³ underneath the research site, which impedes the influences of pumping on the near-surface water. Besides, the pumping rate and the distances from pumping wells to the wetland also reduce the influences from pumping and irrigation.

Using the simulated water table to propose the wetland proved to be an effective method. The wetland extent predicted using MODFLOW was consistent with field observations of hydric soil extent.

5.4 Recommendation

This study confirmed the initial hypothesis that river stage of the Rio Grande controlled water table fluctuations. Further work should include collecting onsite ET data, precipitation data, accurate pumping rate data, installation of additional wells to measure the hydraulic conductivity of the deeper layers, as well as river stage and river bed conductivity near the site.

We make the following observations:

(1) River stage is interpolated from the gauge stations, which are very far from the research site. Considering the surface evaporation, groundwater interactions, and the importance of the river stage on the wetland groundwater elevations, adding a stream gauge station near the study site seems warranted.

(2) Hydraulic conductivity was obtained from the model calibration, for lack of data. A series of pumping tests should be done in the different layers to measure the hydraulic conductivities.

(3) The river bed conductivity was obtained from prior research (Cardenas, 2006). The range of the riverbed conductivity for the site varied from 6.4 m/d to 12.8 m/d. The test location was at the Escondida transect which is about 11km away from Bosquecito. Measuring riverbed conductivity near the site is recommended.

(4). ET and precipitation are from the RAWS station situated in the Bosque del Apache, which could be different from the study site. Bosque del Apache is approximately 24 km from the research site, and the elevation difference is 37 m.

(5) The pumping rate used to irrigate the fields on the west side of the study area was estimated in this model. Preferably measured pumping rate should be used.

(6) A finer DEM should be used in order to better predict the groundwater table, since the groundwater table changes are very subtle for this site.

(7) The model should be further tested by seeing if it could predict water table fluctuations over longer time periods.

REFERENCES

- Anderholm, S. K., Hydrogeology of the Socorro and La Jencia Basins, Socorro County, New Mexico, U.S. Geological Survey Water-Resources Investigations Report 84-4342, 1987
- Alaghmand, S., Beecham, S., Jolly, I. D., Holland, K. L., Woods, J. A., Hassanli, A. Modelling the impacts of river stage manipulation on a complex river-floodplain system in a semi-arid region. *Environmental modeling & software* 59 (2014) 109-126, 2014
- Blaney, H.F., W.D. Criddle, Determining water requirements for settling water disputes, *Natural Resources Journal*, Vol 4, May 1964
- Bear, J., Dynamics of fluids in porous media, Dover Publications, ISBN 0-486-65675-6, 1972
- Brouwer, C., M. Heibloem, Irrigation water management: irrigation water needs, 1986
- Boswell, J.S., G.A. Olyphant, Modeling the hydrologic response of groundwater dominated wetlands to transient boundary conditions: implications for wetland restoration, *Journal of hydrology* (2007) 332, 467-476, 2007
- Bosland, P.W., S. Walker, Growing chiles in New Mexico, Guide H-230, 2014
- Cardenas, M.B.R., Dynamics of fluids, heat and solutes along sediment-water interfaces: a multiphysics modeling study, New Mexico Tech, Doctorate thesis, August 2006
- Dockter, D., Computation of the 1982 Kimberly-Penman and the Jensen-Haise evapotranspiration equations as applied in the U.S. Bureau of Reclamation's Pacific Northwest AgriMet Program, February 1994
- Freeze, R.A., J.A. Cherry, Groundwater. Prentice-Hall, Inc. Englewood Cliffs, NJ, 1979

Feng, X. Q. , Zhang, G. X., Xu, Jun. Y., Simulation of hydrological processes in the Zhalong wetland within a river basin, Northeast China, *Hydrol. Earth Syst. Sci.*, 17, 2797-2807, 2013

Gerla, P. J., Estimating the ground-water contribution in wetland using modeling and digital terrain analysis, *Wetlands*. Vol. 19, No. 2, June 1999. pp394-402, 1999

Gorbach, C., WRRI conference proceedings, 1999

Hvorslev, M.J., Time lag and soil permeability in groundwater observations, April 1951

Hink, V. C., R. D. Ohmart, Middle Rio Grande biological survey, Final Report, 1984

Hattermann, F. F., Krysanova, V., Habeck, A., Bronstert, A., Integrating wetlands and riparian zones in river basin modeling, *Ecological modeling* 199 (2006) 379-39, 2006

I. Joris, J. Feyen. Modelling water flow and seasonal soil moisture dynamics in an alluvial groundwater-fed wetland. *Hydrology and Earth System Sciences Discussions*, Copernicus Publications, 2003, 7 (1), pp.57-66. <hal-00304755>, 2003

Johnson, A.I., Specific yield-compilation of specific yields for various materials, U.S. Geological Survey Open-File Report, 1963

Krause, S., A. Bronstert, An advanced approach for catchment delineation and water balance modeling within wetlands and floodplains, *Advances in geosciences*, 5, 1-5, 2005

Kazezyilmaz-Alhan, C.M., Medina Jr, M. A., Richardson, C. J., A wetland hydrology and water quality model incorporating surface water/groundwater interactions, *WATER RESOURCES RESEARCH*, VOL. 43, W04434, doi:10.1029/2006WR005003, 2007

Karan, S., Engesgaard, P., Looms, M.C., Laier, T., Kazmierczak, J., Groundwater flow and mixing in a wetland-stream system: Field study and numerical modeling, *Journal of hydrology*, 488(2013) 73-83, 2013

Lyon, J.G., L. K. Lyon, Practical Handbook for wetland identification and delineation, Second Edition, CRC Press, 2011

Labbassi, K., Akdim, N., Alfieri, S. M., Menenti, M., Multisource EO data for the optimal agricultural drainage water management in the semiarid area of Doukkala (western Morocco): Potential of sentinel-2 type observation, 2013

McDonald, M.G., A.W. Harbaugh, A modular three-dimensional finite-difference ground-water flow model, Scientific Publications Co, 1988

Majumdar, S.K., Brooks, R.P., Brenner, F.J., Tiner, R.W., Wetlands ecology and conservation: emphasis in Pennsylvania, The Pennsylvania Academy of Science, 1989

Malone, K., H. Williams, Growing season definition and use in wetland delineation, August 2010

Miller, A., Bosquecito water table and hydric soil study interim report, 2011

New Mexico Bureau of Geology and Mineral Resources, Geological map of New Mexico, 1:500,000: New Mexico Bureau of Geology and Mineral Resources, 2003

National Technical Committee for Hydric Soils, The hydric soil technical standard, 2007

New Mexico Environment Department Surface Water Quality Bureau Wetlands Program, New Mexico wetlands technical guide #1 wetland function, 2012

Obropta, C., Kallin, P., Mak, M., Ravit, B., Modelling urban wetland hydrology for the restoration of a forested riparian wetland ecosystem, Urban Habitats, volume 5, number 1, 1541-7115, 2008

Palacios-Velez, E., H. Flores-Magdaleno, Crop evapotranspiration estimation through the use of satellite images, Journal of Earth Science and Engineering 3 (2013) 663-671, 2013

Pessarakli, M., Hand book of plant and crop physiology, third edition, 2014

Rorabaugh, M. I., Estimating changes in bank storage and groundwater contribution to streamflow, 1964

Rango, A., Snow: the real water supply for the Rio Grande basin, New Mexico Journal of Science, Vol. 44, August 2006

Richards, K. E., Hydrologic response of the shallow groundwater to a flood event along the San Acacia reach of the Rio Grande, NM, New Mexico Tech, master thesis, 2006

Springer, R. K., L. W. Gelhar, Charaterization of large-scale aquifer heterogeneity in glacial outwash by analysis of slug tests with oscillatory responses, Cape Cod, Massachusetts. U.S. Geol. Survey Water Resources Investigation Report 91-4034, 1991

Schulze-Makuch, D., Carlson, D., Cherkauer, D., Malik, P., Scale dependency of hydraulic conductivity in heterogeneous media, Groundwater 37 (6), 904-919, 1999

Spane, F.A., Considering barometric pressure in groundwater flow investigations, Water Resources Research, Vol 38, Is 6, 1944-7973, 2002

S.S. Papadopoulos & Associates, Inc. Technical memorandum exploratory and shallow well drilling middle Rio Grande watershed study-Phase 1, 2003

Shafike, N. G., Linked surface water and groundwater model for San Acacia reach as a tool to support decision making analysis, Identifying Technologies to Improve Regional Water Stewardship: North-Middle Rio Grande Corridor 21-22 April 2004

Shah, N., Nachabe, M., Ross, M., Extinction depth and evapotranspiration from ground water under selected land covers, Ground Water, Vol. 45, No. 3, May-June 2007

Siegle, R., Reed, G., Moore, D., Bosque del Apache sediment plug baseline studies, U.S. Department of the Interior Bureau of Reclamation, Annual Report, 2010

Toth, J., A theoretical analysis of groundwater flow in small drainage basins, Journal of geophysical research, Vol. 68, No. 16, August 1963

U.S. Army Corps of Engineers, Technical standard for water-table monitoring of potential wetland sites, June 2005

Vasilas, L. M., Hurt, G. W., Noble, C. V. United States Department of Agriculture, Natural Resources Conservation Service. 2010. Field indicators of hydric soils in the United States, Version 7.0. USDA, NRCS, in cooperation with the National Technical Committee for Hydric Soils, 2010

Wilcox, L.J., Telescopic model of groundwater and surface water interactions near San Antonio, NM, New Mexico Tech master thesis, 2003

Zhong, P., Yang, Z. F., Cui, B. S., and Liu, J. L., Studies on water resource requirement for eco-environmental use of the Baiyangdian Wetland, Acta Sci. Circumst., 25, 1119-1126, 2005